COMPARISON OF THREE ANALYTICAL TECHNIQUES FOR GENERAL CHARACTERISATION OF SELECTED ALGAE AND CYANOBACTERIA

SUHAINA NASHATH BINTI MOHAMED IQBAL

FACULTY OF SCIENCE
UNIVERSITI MALAYA
KUALA LUMPUR

2020

COMPARISON OF THREE ANALYTICAL TECHNIQUES FOR GENERAL CHARACTERISATION OF SELECTED ALGAE AND CYANOBACTERIA

SUHAINA NASHATH BINTI MOHAMED IQBAL

DISSERTATION SUBMITTED IN FULFILMENT OF THE REQUIREMENTS FOR THE DEGREE OF MASTER OF SCIENCE

INSTITUTE OF BIOLOGICAL SCIENCES
FACULTY OF SCIENCE
UNIVERSITI MALAYA
KUALA LUMPUR

2020

UNIVERSITI MALAYA

ORIGINAL LITERARY WORK DECLARATION

Name of Candidate: **SUHAINA NASHATH BINTI MOHAMED IQBAL**

Matric No: **SGR160058**

Name of Degree: **MASTER OF SCIENCE**

Title of Dissertation ("this Work"):

COMPARISON OF THREE ANALYTICAL TECHNIQUES FOR GENERAL CHARACTERISATION OF SELECTED ALGAE AND CYANOBACTERIA Field of Study: **BIOTECHNOLOGY**

I do solemnly and sincerely declare that:

(1) I am the sole author/writer of this Work;
(2) This Work is original;
(3) Any use of any work in which copyright exists was done by way of fair dealing and for permitted purposes and any excerpt or extract from, or reference to or reproduction of any copyright work has been disclosed expressly and sufficiently and the title of the Work and its authorship have been acknowledged in this Work;
(4) I do not have any actual knowledge nor do I ought reasonably to know that the making of this work constitutes an infringement of any copyright work;
(5) I hereby assign all and every rights in the copyright to this Work to the Universiti Malaya ("UM"), who henceforth shall be owner of the copyright in this Work and that any reproduction or use in any form or by any means whatsoever is prohibited without the written consent of UM having been first had and obtained;
(6) I am fully aware that if in the course of making this Work I have infringed any copyright whether intentionally or otherwise, I may be subject to legal action or any other action as may be determined by UM.

Candidate's Signature Date:

Subscribed and solemnly declared before,

Witness's Signature Date:

Name:

Designation:

COMPARISON OF THREE ANALYTICAL TECHNIQUES IN GENERAL CHARACTERISATION OF SELECTED ALGAE AND CYANOBACTERIA

ABSTRACT

Algae and cyanobacteria maintain the oxygenation of earth, and are utilised as biofuels, biofertilizers and nutrition feed. The characterisation of algae and cyanobacteria through conventional methods require technical expertise, laborious sample preparation, and moderately expensive instruments and reagents. Hence, in this study, selected bioanalytical techniques with minimal sample preparation were incorporated, to simplify the characterisation of algae and cyanobacteria. The objectives of this research were to study the phylogenetic relationship of the selected algae and cyanobacteria via the 23S plastid ribosomal ribonucleic acid (rRNA) and 18S rRNA biomarkers; to validate the presence of the microcystin synthetase (mcy) gene cluster encoding the biosynthesis of microcystin in the selected cyanobacteria; to identify the organic compounds present in the selected algae and cyanobacteria via gas chromatography-mass spectrometry (GC-MS); and to study the vibrational properties exhibited by the atom of the selected algae and cyanobacteria via Raman spectroscopy. Pure cultures of the selected algae and cyanobacteria were sourced from the culture collection centre. The deoxyribonucleic acid (DNA) of algae and cyanobacteria was extracted following the phenol-chloroform protocol, and subjected to the polymerase chain reaction (PCR) using the 23S plastid rRNA (p23SrV) biomarker. The taxonomic clade of brown algae (*Chaetoceros calcitrans* and *Isochrysis galbana*), green algae (*Chlorella* spp. and *Tetraselmis* spp.), and cyanobacteria (*Microcystis aeruginosa* and *Nostoc* spp.), were distinguished. This universal biomarker simplified the taxonomic classification of both algae (eukaryotic) and cyanobacteria (prokaryotic). Whereas, the 18S rRNA (18Sr) biomarker shows a further separation of *C. calcitra*ns and *I. galbana* into two different clades, and green algae as a single clade. Furthermore, the mcy gene cluster was not expressed in both of

the cyanobacteria species. In addition, in GC-MS analysis, the organic phase of algae and cyanobacteria was extracted via solvent extraction, prior to injecting in the Agilent 6890N Network GC system. The organic compounds, namely alkane, alkyne, alcohol, phenol, polycyclic hydrocarbon, aromatic ketone, and siloxane were eluted, based on its polarity and volatility properties. These compounds are bio-commercialised as biofuels, cosmetics and skincare, industrial polymers and lubricants, paint coatings, and paraffin waxes. Lastly, a thin film of air-dried algae and cyanobacteria were analysed in Renishaw In Via Raman Microscope. The Raman spectra produced corresponded with saffron and carotene photosynthetic pigments, at peaks 1010 cm^{-1}, 1155 cm^{-1} and 1520 $cm-^{1}$. These pigments can be extracted from algae and cyanobacteria, and bioengineered for industrial use. Briefly, this research serves as a baseline study for environmental monitoring and a quick approach to identify compounds, that are beneficial as biofuels and pharmaceutical products in the future. Freshwater algae and cyanobacteria could be a fundamental source for farmers to harvest, and convert waste materials to useful materials. Algae blooms which are potential biotoxins for fishes and prawns, can now be converted sustainably, in-line to convert waste to wealth strategy.

Keywords: Algae and cyanobacteria, p23SrV, microcystin, GC-MS, Raman spectroscopy.

PERBANDINGAN TIGA TEKNIK ANALITIKAL UNTUK KARAKTERISASI UMUM ALGA DAN SIANOBAKTERIA TERPILIH

ABSTRAK

Alga dan sianobakteria mengekalkan pengoksigenan bumi, dan memberi manfaat seperti bio bahan api, bio baja, dan sumber pemakanan. Pencirian alga dan sianobakteria melalui kaedah konvensional memerlukan kepakaran teknikal, penyediaan sampel yang sukar, serta instrumen dan reagen yang mahal. Oleh itu, dalam kajian ini, teknik bioanalitikal terpilh dengan penyediaan sampel yang minimum telah digunakan, untuk memudahkan pencirian alga dan sianobakteria. Objektif penyelidikan ini adalah untuk mengkaji hubungan filogenetik antara alga dan sianobakteria terpilih melalui penanda 23S plastid asid ribonukleik ribosom (rRNA) dan 18S rRNA; untuk mengesahkan kehadiran kluster gen 'microcystin synthetase' (mcy) yang mengekodkan biosintesis 'microcystin' dalam sianobakteria terpilih; untuk mengenal pasti sebatian organik yang terdapat dalam alga dan sianobakteria terpilih melalui spektrometri massa-kromatografi gas (GC-MS); dan untuk mengkaji sifat-sifat getaran yang dipamerkan oleh atom alga dan sianobakteria terpilih melalui spektroskopi Raman. Kultur tulen alga dan sianobakteria terpilih telah diperolehi dari pusat koleksi kultur. Asid deoksiribonukleik (DNA) alga dan sianobakteria telah diekstrak mengikut protokol fenol-kloroform, dan diuji dalam tindak balas rantai polimer (PCR) dengan menggunakan penanda 23S plastid rRNA (p23SrV). Klad taksonomi alga coklat (*C. calcitrans* dan *I. galbana*), alga hijau (*Chlorella* spp. dan *Tetraselmis* spp.) dan sianobakteria (*M. aeruginosa* dan *Nostoc* spp.), dibezakan. Penanda sejagat ini telah memudahkan klasifikasi taksonomi kedua-dua alga (eukaryotik) dan sianobakteria (prokaryotik). Manakala, penanda 18S rRNA (18Sr) menunjukkan pemisahan di antara *C. calcitrans* dan *I. galbana* ke dalam dua klad yang berbeza, dan alga hijau sebagai satu klad tunggal. Tambahan pula, kluster gen mcy tidak diekspres dalam kedua-dua spesies sianobakteria. Di samping itu, dalam analisis GC-MS, fasa

organik alga dan sianobakteria telah diekstrak melalui pengekstrakan pelarut, sebelum dianalisis dalam ‘Agilent 6890N Network GC system’. Sebatian organik, iaitu alkana, alkina, alkohol, fenol, hidrokarbon polisiklik, keton aromatic, dan siloksan telah dikesan, berdasarkan sifat kekutuban dan volatilnya. Sebatian ini bio-dikomersilkan sebagai bio bahan api, kosmetik dan penjagaan kulit, polimer dan pelincir perindustrian, salutan cat, dan lilin parafin. Akhir sekali, filem nipis alga dan sianobakteria kering dianalisis dalam ‘Renishaw In Via Raman Microscope’. Spektra Raman yang dihasilkan dikaitkan dengan pigmen fotosintesis kunyit dan karoten, di puncak 1010 cm^{-1}, 1155 cm^{-1} and 1520 cm^{-1}. Pigmen ini boleh diekstrak daripada alga dan sianobakteria, dan diaplikasikan untuk kegunaan perindustrian. Secara ringkasnya, penyelidikan ini berfungsi sebagai kajian dasar untuk pemantauan alam sekitar dan pendekatan cepat untuk mengenal pasti sebatian, yang bermanfaat sebagai bio bahan api dan produk farmaseutikal pada masa hadapan. Alga dan sianobakteria air tawar boleh menjadi sumber asas bagi petani untuk menuai, dan menukar bahan buangan kepada bahan yang berguna. Pertumbuhan alga mekar yang berpotensi sebagai biotoksin dalam ikan dan udang, kini boleh ditukar secara mampan, dengan menukar sisa kepada strategi kekayaan.

Kata Kunci: Alga dan sianobakteria, p23SrV, GC-MS, ‘microcystin’, spektroskopi Raman.

ACKNOWLEDGEMENTS

First and foremost, all praise to the Almighty Allah, for His blessings, in providing me with the opportunities and strength to accomplish this research. My deepest gratitude to my supervisor, Professor Dr. Subha Bhassu, for her invaluable guidance, constructive suggestions, and warm encouragement throughout this research. A special thanks to my parents for financial aids and unconditional support through good and bad times.

Besides, I would like to extend my sincere appreciation to Ms Farhana Abd Wahid and Ms Radziah Saarani, the scientific officers of Nanotechnology and Catalysis Research Centre, for their kind help in performing the GC-MS and Raman spectroscopy analysis. I am grateful to the laboratory assistants of the Centre for Research in Biotechnology for Agriculture (CEBAR), and the Department of Genetics and Molecular Biology, for allowing me to use their laboratory facilities and chemicals.

Apart from that, I would like to express my heartfelt dedication to Professor Dr. Mohamed Shariff Mohamed Din and his research associates, from Universiti Putra Malaysia, for their great contributions in providing the algae cultures. A big thanks to MyTACG Bioscience Enterprise for their reliable sequencing and bioinformatics analysis service. I would like to thank my beloved AGAGEL lab mates and all my friends, for their precious help in assisting with the experiments, proofreading and moral support.

The financial support provided by the CEBAR research grants was greatly appreciated. Finally, I am gratified to everyone who lent their hand in this venture, directly or indirectly, that eventually driven me to produce this final masterpiece.

TABLE OF CONTENTS

LIST OF FIGURES

LIST OF TABLES

LIST OF SYMBOLS AND ABBREVIATIONS

Å	:	Angstrom
°C	:	Degree Celsius
eV	:	Electron volt
cm^{-1}	:	Frequency
g	:	Gram
kg	:	Kilogram
L	:	Litre
m/z	:	Mass-to-charge ratio
µg	:	Microgram
µl	:	Microlitre
mA	:	Milliampere
mg	:	Milligram
ml	:	Millilitre
mM	:	Millimolar
M	:	Molar
ng	:	Nanogram
nm	:	Nanometre
%	:	Percentage
V	:	Voltage
v/v	:	Volume per volume
w/v	:	Weight per volume
Adda	:	3-amino-9-methoxy-2,6,8-trimethyl-10-phenyl-4,6-decadienoic acid
BG11	:	Blue-green medium

BLAST	:	Basic local alignment search tool
bp	:	Base pair
CCAP	:	Culture Collection of Algae and Protozoa
CTAB	:	Cetyltrimethylammonium bromide
D-MeAsp	:	3-methylaspartic acid
DNA	:	Deoxyribonucleic acid
DnaSP	:	DNA sequence polymorphism
dNTP	:	Deoxynucleoside triphosphate
ECHA	:	European Chemicals Agency
EDTA	:	Ethylenediaminetetraacetic acid
ELISA	:	Enzyme-linked immunosorbent assays
GC-MS	:	Gas chromatography-mass spectrometry
HAB	:	Harmful algal bloom
HPLC	:	High-performance liquid chromatography
hr	:	Hour
IR	:	Infrared
ITS	:	Internal transcribed spacer
LD_{50}	:	Lethal dose
mcy	:	Microcystin synthetase
Mdha	:	N-methyl-dehydroalanine
MEGA7	:	Molecular Evolutionary Genetics Analysis version 7.0
min	:	Minute
NaCl	:	Sodium chloride
NCBI	:	National Center for Biotechnology Information
NMT	:	N-methyltransferase
NRPS	:	Nonribosomal peptide synthetase

ORFs	:	Open reading frames
ppt	:	Parts per thousand
PCR	:	Polymerase chain reaction
PKS	:	Polyketide synthetase
PVC	:	Polyvinylchloride
psi	:	Pound-force per square inch
rpm	:	Revolutions per minute
rRNA	:	Ribosomal ribonucleic acid
SDS	:	Sodium dodecyl sulfate
Si	:	Silicon
TAE	:	Tris base/Acetic acid/EDTA
TE	:	Tris/EDTA
UV	:	Ultraviolet
WiRE	:	Windows-based Raman Environment

LIST OF APPENDICES

CHAPTER 1: INTRODUCTION

1.1 Background of the Study

Algae and cyanobacteria have a major role in the photosynthetic activity of an aquatic ecosystem, as the primary producer. Algae are cultivated as aquaculture feeds (Abd Rahman et al., 2018; Abdu Rahman et al., 2017; Mohebbi et al., 2016) and biofertilizers (Abdel-Raouf et al., 2012). Nevertheless, cyanobacteria after excessive blooms, may release cyanotoxins, which biomagnifies, and causes mortality in the aquatic species (Ettoumi et al., 2011; Ferrão-Filho & Kozlowsky-Suzuki, 2011; Smith et al., 2008). The characterisation of algae and cyanobacteria are important to determine the species heredity in taxonomy, to identify the toxic strains for food safety, and to characterise the organic compound by-products for industrial commercialisations.

The conventional analytical technique for the characterisation of algae and cyanobacteria comprises of microscopic imaging, immunohistochemical staining, enzyme-linked immunosorbent assays (ELISA), flow cytometry, x-ray crystallography and chromatography analysis (Kaur et al., 2018; Ahmed et al., 2014; Fischer et al., 2000). The main shortcomings of engaging these characterisation techniques are that; it requires lengthy sample preparation, the chemicals and the antibodies utilised are relatively expensive, and technician expertise's are needed for instruments operation (Hosseini et al., 2018; Ahmed et al., 2014; Alunni-Fabbroni & Sandri, 2010; Fournier et al., 2013).

The selected bioanalytical techniques that simplify the characterisation of algae and cyanobacteria were discussed in this study. The conventional primers, namely 16S rRNA, 18S rRNA and internal transcribed spacer (ITS) gene region were commonly incorporated in gene amplification of algae and cyanobacteria (Premanandh et al., 2006;

Connell, 2002; Friedl & O'Kelly, 2002; Fiore et al., 2000), as it was a challenge to develop a universal primer, up until the study by Sherwood & Presting (2007) and Presting (2006). Their studies utilised the p23SrV biomarker as a universal primer, in targeting the conserved region of cyanobacteria and plastids of algae. Hence, these primers were utilised in this study. In addition, cyanotoxins (microcystin, the most common) are released during the blooming of cyanobacteria. The presence of the mcy gene clusters encoding the biosynthesis of microcystin was validated in this study.

Besides, GC-MS is an excellent analytical tool for environmental testing, as it can identify and quantify the organic materials produced by algae and cyanobacteria (Shakeel et al., 2015; Furuhashi & Weckwerth, 2013). The effect of these organic compounds to the aquatic environment was studied. Furthermore, Raman spectroscopy is based on the inelastic scattering (Raman scattering) of photons. The vibrational effect of an atom during the excitation of electrons (Lin-Vien et al., 1991) produce fingerprinting characteristics that are essential in this study. Both techniques have several advantages; rapid signal detection, direct sample assessment and minimal sample preparation time (Jehlička et al., 2014), which favours over the conventional analytical assays.

Briefly, this study focuses on the selected bioanalytical approaches that facilitate the detection and characterisation of algae and cyanobacteria, for the benefits of the aquaculture farmers. The simplified approaches in this study can be applied for the rapid identification of algae and cyanobacteria blooms, and its associated organic compounds can be bioprocess for industrial applications. As algae and cyanobacteria play a crucial role in the oxygenation of earth and provide many ecological benefits, mankind should never overlook their existence.

1.2 Problem Statement

Multiple primer sets that are utilised for the taxonomic classification of algae and cyanobacteria, in previous studies, may result in false positives (Ma et al., 2011). The molecular biomarker utilised in this study may eradicate this dispute, as the characterisation of both prokaryote and eukaryote can be achieved with this single universal primer. Besides, there are limited studies on the inelastic scattering of Raman spectroscopy, as the resulting vibrational properties are fingerprinting or unique in each algae and cyanobacteria. The conventional analytical assays have drawbacks such as laborious sample preparation, and expensive chemicals and machinery maintenance (Hosseini et al., 2018; Ahmed et al., 2014). Hence, selected bioanalytical techniques with simplified extraction protocol were investigated in this study, for quick identification of algae and cyanobacteria species, and its associated novel organic compounds.

1.3 Research Objectives

The research objectives of this study are as follows;

1. To study the phylogenetic relationship of the selected algae and cyanobacteria via the p23SrV and 18Sr biomarkers.
2. To validate the presence of the mcy gene cluster encoding the biosynthesis of microcystin in the selected cyanobacteria.
3. To identify the organic compounds present in the selected algae and cyanobacteria via GC-MS.
4. To study the vibrational properties exhibited by the atoms of the selected algae and cyanobacteria via Raman spectroscopy.

1.4 Overview of the Dissertation

This dissertation is comprised of six chapters, described as following.

Chapter 1, the introduction explained the background of the study, the problem statement, the research objectives, and the overview of the dissertation.

Chapter 2, a comprehensive literature review describing the following topic. The biology and characteristics of algae and cyanobacteria; the importance of algae; the types of cyanotoxins produced; the cyanotoxins poisoning and its mitigation strategies; the mcy gene cluster; the drawbacks of conventional analytical assays; and the selected analytical techniques for the characterisation of algae and cyanobacteria comprising of the p23SrV biomarker; GC-MS, and Raman spectroscopy.

Chapter 3, the research methodology. The research design and the analytical methods employed for the characterisation of the selected algae and cyanobacteria, were described.

Chapter 4, the results. The phylogenetic relationships using the p23SrV and 18Sr biomarkers, the mcy gene cluster in the biosynthesis of microcystin, the detection of organic compounds using the GC-MS, and the vibration properties of the atoms using the Raman spectroscopy, were analysed.

Chapter 5, the discussion. The findings and the outcome of the study were discussed in detail, comparing with the previous literature studies.

Chapter 6, the conclusion. The summary of the findings, the limitation of the study, and the recommendations for future work, were emphasised in this final chapter.

CHAPTER 2: LITERATURE REVIEW

2.1 Algae

2.1.1 Biology and Characteristics

Algae are a diverse group of eukaryotic organisms and are classified as Protista. The major groups of algae consist of green algae, red algae, brown algae, diatom and dinoflagellates (Raven et al., 1999; Lembi & Waaland, 1988). Another group is cyanobacteria or widely known as blue-green algae, but they are not considered true algae as they are prokaryotes (Raven et al., 1999; Lembi & Waaland, 1988).

Algae are unicellular or multicellular and range from microscopic to macroscopic in size. Algae are found in the freshwater or marine environment, appearing as colonies, patches, filamentous, or leafy. Most algae reproduce asexually via fragmentation, binary fission, budding and spores. In sexual reproduction, the life cycle varies between different species of algae. They exhibit alternation of generations, which consist of gametophyte and sporophyte generation (Raven et al., 1999; Lembi & Waaland, 1988).

Brown algae; *C. calcitrans* and *I. galbana*, are classified under Kingdom Chromista, and possess chlorophyll-a, chlorophyll-c, and accessory pigments such as carotene and xanthophyll (Maneveldt & Keats, 2003). The food is stored in the chrysolaminarin vesicles outside of chloroplast (Gould et al., 2008; Maneveldt & Keats, 2003). Meanwhile, green algae; *Chlorella* spp. and *Tetraselmis* spp., are classified under Kingdom Plantae, and possess chlorophyll-a, chlorophyll-b and accessory pigments.

C. calcitrans is a centric diatom, with silica frustules connecting to thin setae, to form a colony of cells (Maneveldt & Keats, 2003). *I. galbana* is globular and lacks flagella (Maneveldt & Keats, 2003). It has the highest amount of fucoxanthin (Kim et al., 2012b), which has anti-inflammatory and antioxidant properties (Zhang et al., 2015). *Tetraselmis* spp. is ovoid, with an eyespot and flagella for motion (Norris et al., 1980).

2.1.2 Importance of Algae

Algae play a central role as the major primary producer in an aquatic ecosystem. *Nannochloropsis* spp. is used as nutrition feeds in fish larvae (Spolaore et al., 2006). Artificial fish feeds are mixed with algae to give extra nutrients in juvenile invertebrates, fishes and crustaceans (Spolaore et al., 2006). *Chlorella* spp. and *Spirulina* spp. are used as food supplements; as it helps in the gut detoxification, reduces cholesterol and blood pressure, and provides an energy boosts (Abdel-Raouf et al., 2012).

Algae are grown in minimal need for water source and are tolerable to extreme environments (Abdel-Raouf et al., 2012; Demirbas & Demirbas, 2011). Algae are extremely important as a source of biofuels, which could potentially replace fossil fuel. Half of the composition of algae is made up of lipid oil, and the yield of algae oil is almost 30 times higher than the palm oil (Furuhashi & Weckwerth, 2013; Demirbas & Demirbas, 2011). Hence, suitable to be bioprocessed as biofuels for cars, trucks and aeroplanes.

In addition, algae are used as biofertilizers and soil stabilizers in agriculture (Abdel-Raouf et al., 2012). Algae as biofertilizer, reduce phosphorus and nitrogen run-off to the rivers, thus, water quality increases (Abdel-Raouf et al., 2012). The growth of *Chlorella* spp. in wastewater reduces phosphorus, nitrogen, and heavy metals such as aluminium, calcium, iron, magnesium and manganese (Abdel-Raouf et al., 2012; Wang et al., 2009).

2.2 Cyanobacteria

2.2.1 Biology and Characteristics

Cyanobacteria is one of the earliest microorganisms that has lived since 3500 million years ago (Whitton & Potts, 2012). It is initially identified as algae and later reclassified as eubacteria (Buchanan & Gibbons, 1974). Despite being classified as a gram-negative bacterium, the term 'blue-green algae' is still prevalent to several researchers to date, due to its magnificent role in synthesising chlorophyll-a, and maintaining the oxygenation of the biosphere and the biogeochemical cycles (Blank & Sanchez-Baracaldo, 2010).

Cyanobacteria appear in diverse forms from simple unicellular to complex filamentous (Ishida et al., 2001). Cyanobacteria is hardy, as it can withstand high ultraviolet (UV) exposure and fluctuating temperatures (Ferrao-Filho & Kozlowsky-Suzuki, 2011). *M. aeruginosa*, *Nostoc* spp., *Nodularia* spp., *Anabaena* spp. and *Cylindrospermopsis* spp., are some of the well-known species of cyanobacteria. *M. aeruginosa* is spherical, while, *Nostoc* spp. is barrel-shaped connected in filaments. All cyanobacteria possess chlorophyll-a, and phycobilin (phycocyanin, accounting for its bluish-green appearance or phycoerythrin, a red photosynthetic pigment) (Whitton & Potts, 2012).

Furthermore, heterocyst, a specialised nitrogen-fixing cell supplies nitrogen to the vegetative cells, catalysed by the enzyme nitrogenase (Kumar et al., 2010). Heterocyst also produces akinetes, which is dormant in the harsh environment until suitable conditions are available for germination (Adams & Duggan, 1999). The vacuoles are comprised of gas vesicles for buoyancy control and vertical drifting in the water column, in response to light and nutrients (Brookes & Ganf, 2001). Although cyanobacteria provide numerous ecological benefits, toxic secondary metabolites are produced during excessive blooms, which harms the environment and the consumers.

2.2.2 Types of Cyanotoxins

Cyanobacteria produce cyanotoxins as secondary metabolites, which are classified into hepatotoxins (microcystin, nodularin and cylindrospermopsin), neurotoxins (anatoxin, saxitoxin and β-Methylamino-L-alanine) and dermatoxins (lyngbyatoxin, lipopolysaccharide and aplysiatoxin) (Ettoumi et al., 2011; Smith et al., 2008). Aquatic animals exposed to cyanotoxins undergo biochemical and behavioural changes, reduced feeding intake, stagnant growth and fecundity, paralysis and mortality (Ferrao-Filho & Kozlowsky-Suzuki, 2011).

Microcystin and nodularin causes liver damage in the hepatopancreas of sea trout, disrupts the osmoregulation in estuarine crab, and inhibits the protein phosphatase and sodium channels activity (Ettoumi et al., 2011; Smith et al., 2008). Cylindrospermopsin damages the liver, kidney and adrenal glands, inhibits the protein synthesis, and causes mortality in brine shrimps (Ettoumi et al., 2011; Smith et al., 2008; Falconer & Humpage, 2006). Lyngbyatoxin causes intestinal bleeding, stomach ulcers and death in mice (Ettoumi et al., 2011; Smith et al., 2008).

Anatoxin and saxitoxin block the acetylcholinesterase activity and the nerve cells of sodium channels, resulting in abnormal swimming and mortality of fishes and daphniids (Ettoumi et al., 2011; Smith 2008). Cyanobacteria inhabiting in the roots of cycad trees produce β-Methylamino-L-alanine, causing amyotrophic lateral sclerosis, a neurological disorder (Ettoumi et al., 2011; Murch et al., 2004; Banack & Cox, 2003; Monson et al., 2003). Cyanotoxins may remain in the tissues and biomagnifies via the food chain or dietary exposure in humans (Rastogi et al., 2014).

2.2.3 Cyanotoxins Poisoning and Its Mitigation Strategies

An outbreak of acute liver failure attributed to Caruaru syndrome was reported in Caruaru, Brazil. The patients experienced poor vision and nausea, after the routine haemodialysis. Eventually, three-quarters of them were dead from acute liver failure (Carmichael et al., 2001). Phytoplankton examination, water treatment analysis and liver biopsy verified that microcystin and cylindrospermopsin were detected in the water sample, at 19.5 µg/L (Carmichael et al., 2001).

Harmful algal bloom (HAB) is a phenomenon caused by the bloom of algae, producing biotoxins. HAB has been reported in Kelantan, Sabah, Sarawak and Johor in the past decade, especially during the red tide season by the dinoflagellate, *Alexandrium* spp., and other harmful algae (Lim et al., 2012). HAB could result in water discolouration, fish kills, and hospitalisation due to shellfish poisoning (Watson et al., 2015; Lim et al., 2012).

Sim (2015) has reported several effective ways of removing cyanobacteria blooms. For instance, the mixing of artificial water destroys the stratified layer of the water column and the buoyancy of cyanobacteria. The addition of copper sulphate and hydrogen peroxide results in the inhibition of photosynthesis, phosphorus and nitrogen fixation, leading to the elimination of cyanobacteria. The grazing activities of copepods and daphnia or the introduction of cyanophage and lytic bacteria also eliminate the blooms.

However, the drawback of incorporating these methods introduces invasive species into the ecosystem, harming the non-target species (Sim, 2015). Hence, to minimise the impact of HAB's, the assessment on aquaculture farms such as hydrography, flocculation and phytoplankton assemblages, are taken into considerations (Lim et al., 2012).

2.2.4 mcy Gene Cluster

Microcystin is one of the families of hepatotoxins, with 70 different isomers, that is commonly produced by *M. aeruginosa*, *Nostoc* spp., *Anabaena* spp. and *Planktothrix agardhii*. The chemical structure of this potent cyclic heptapeptides consists of Adda (3-amino-9-methoxy-2,6,8-trimethyl-10-phenyl-4,6-decadienoic acid), D-Glutamate, Mdha (N-methyl-dehydroalanine), D-Alanine, L-X, D-MeAsp (3-methylaspartic acid) and L-Z. X and Z are the L-amino acids that are variable in different isomers of microcystin (Neilan et al., 2008; Mikalsen et al., 2003; Tillett et al., 2000).

The biosynthesis of microcystin is via a mixed nonribosomal peptide synthetase (NRPS) and polyketide synthetase (PKS) enzymatic pathway. The size of the mcy gene cluster is about 55 kb, with 10 transcribed open reading frames (ORFs), arranged bidirectionally in two operons, known as mcyA–C and mcyD–J. The mcyD is a double chain PKS domain, the mcyE and mcyG is a hybrid of NRPS and PKS domain, the mcyA–C is an NRPS domain, and the additional four ORFs (mcyF, mcyH, mcyI and mcyJ) are responsible for the tailoring, modification and transportation of microcystin (Neilan et al., 2008; Dittmann & Borner, 2005; Tillett et al., 2000). The arrangement of the ORFs varies in different species of cyanobacteria (Neilan et al., 2008).

The biosynthesis of microcystin occurs via a series of an enzymatic reaction, starting from the biosynthesis of Adda up until L-Arginine (Neilan et al., 2008; Dittmann & Borner, 2005; Tillett et al., 2000). The NRPS adenylation domain of mcyG catalyses the first step of the formation of Adda, by activating phenylacetate. Subsequent addition of malonyl-CoA and the biosynthesis of PKS domain of mcyG, mcyD and mcyE, elongates phenylacetate. The aminotransferase of mcyE produces D-glutamate, completing the biosynthesis of Adda.

The NRPS of mcyE comprises of two condensation domains, an adenylation domain and a thiolation domain. The formation of peptide bonds occurs in the condensation domain, the first between Adda and D-Glutamate, and the second between D-Glutamate and Mdha. The NRPS of mcyA comprises of two domains of adenylation and thiolation, a condensation domain, an N-methyltransferase (NMT) domain and an epimerisation domain. The adenylation domain then activates L-Serine, followed by D-Alanine, with condensation domain catalysing the peptide bond. The NMT domain allows the specific activation of the first adenylation of mcyA, while, the thiolation and epimerisation domains are involved in the modification of the amino acids.

The growing peptide chain next encounters the NRPS of mcyB and mcyC. There are two domain modules of condensation, adenylation and thiolation, in mcyB, while, only a single domain module with thioesterase domain, in mcyC. The adenylation domain in mcyB activates L-Leucine, followed by D-MeAsp. The activation of D-MeAsp might not occur if the peptide bond between L- and D- amino acid is not catalysed, or if the α-carboxyl group is inactivated (Tillett et al., 2000). Finally, L-Arginine is activated in the adenylation domain of mcyC, and cyclic transformation occurs in the thioesterase domain, releasing microcystin-LR as the final product.

2.3 The Drawbacks of Conventional Analytical Assays

Microscopic imaging has been the most prominent method in quick identification of species morphology, for centuries (Ahmed et al., 2014; Carpenter et al., 2006). Even with the advancement of the microscope, different species may exhibit similar morphological characteristics, obstructing the classification accuracy and specificity (Ahmed et al., 2014). Likewise, basic identification methods such as cell culture and plate count are time-consuming (Lazcka et al., 2007). The propagation of some bacteria or pathogens are very slow, and the usage of specific enrichment media may favour the growth of non-selective organisms, contaminating the cultures (Lazcka et al., 2007).

Biochemical assays, namely ELISA and immunohistochemical staining are expensive and depend on enzymes or antibody that are specific to its expression (Hosseini et al., 2018; Reverté et al., 2014; Pakala & Waksman, 2011). Cross-reactions with the antibodies are highly present and small biomolecules have low binding affinity to the antibodies (Kaur et al., 2018; Hosseini et al., 2018; Ahmed et al., 2014). In flow cytometry, the fluorescence noise produced during the measurement obstructs the characterisation, and massive data are generated which may be unnecessary, while, in x-ray crystallography, the crystallisation technique is challenging (Kaur et al., 2018).

Besides, chromatography analysis such as high-performance liquid chromatography (HPLC) and liquid chromatography-mass spectrometry are widely used in biotoxins screening of microbes for environmental monitoring, delivering a reliable and robust result (Loftin et al., 2010; Rodriguez-Mozaz et al., 2007). Nevertheless, the expensive reagents and chemical standards, the high cost of maintenance of the equipment, the need of specialised technicians, as well as, strenuous sample processing and clean-up protocol, makes it a hassle method to be considered (Rodriguez-Mozaz et al., 2007).

2.4 Selected Analytical Techniques for the Characterisation of Algae and Cyanobacteria

2.4.1 The p23SrV Biomarker

Phylogenetic trees such as Neighbor-Joining tree, Maximum Likelihood or Maximum Parsimony are constructed to study the evolutionary relationships among a group of taxa, either via distance matrix method or evolutionary aspects (Pavlopoulos et al., 2010). Sherwood & Presting (2007) and Presting (2006) have reported that the construction of the Neighbor-Joining tree based on the 23S plastid rRNA gene region, characterised the taxonomic lineage of algae groups (e.g., algae, diatoms, euglenoids) and cyanobacteria. The p23SrV biomarker as a universal primer pair, classified the taxonomic clades of algae groups and cyanobacteria, simultaneously (Sherwood & Presting, 2007; Presting, 2006).

The p23SrV primer pair sequence are as follows; "p23SrV_F1 (5'-GGA CAG AAA GAC CCT ATG AA-3'), and p23SrV_R1 (5'-TCA GCC TGT TAT CCC TAG AG-3')". This conserved region can only be found in plastids and cyanobacteria (Sherwood & Presting, 2007; Presting, 2006). Hence, this region functions as a universal biomarker that is essential for DNA barcoding in different groups of algae and cyanobacteria (Presting, 2006). The conventional primers incorporated in past studies may indicate false-positives due to incorrect binding of primer (Ahmed et al., 2014; Ma et al., 2011). The p23SrV biomarker eradicates this hassle in PCR and simplified the characterisation.

Plastids are originated from cyanobacteria (Deusch et al., 2008) via endosymbiosis. A heterotrophic eukaryote host engulfs a cyanobacteria (primary endosymbiosis), evolving into three lineages of algae; chlorophytes (green algae), rhodophytes (red algae) and glaucophytes, and acquiring two bounded membranes of primary plastids (Cavalier-Smith, 2018; Gould et al., 2008; Nozaki et al., 2004; McFadden, 2001). Subsequently, a

secondary endosymbiosis occurred when another heterotrophic eukaryote host engulfs these algae groups, and acquire three to four bounded membrane (Cavalier-Smith, 2018; Gould et al., 2008; Nozaki et al., 2004; McFadden, 2001).

Secondary endosymbiosis produces the descendants of red algae such as dinophytes, haptophytes, heterokontophytes, and cryptophytes, while, euglenophytes are from green algae (Gould et al., 2008). Further endosymbiosis occurs in other descendants of algae or endosymbiont with cyanobacteria (Gould et al., 2008). The series of endosymbiosis signified the evolution of plastids and increased species complexity (McFadden, 2001).

2.4.2 GC-MS

Algae and cyanobacteria are cultivated extensively as biofuels, as an alternative source to fossil fuels production (Pradana et al., 2017; Sharmila et al., 2016; Furuhashi & Weckwerth, 2013). The biosynthesis of fatty acids and hydrocarbons are the two key components in lipid analysis to produce biofuels (Furuhashi & Weckwerth, 2013), which are characterised in GC-MS. Fatty acid methyl esters extraction comprising of lipophilic extraction and methyl esterification are carried out, prior to GC-MS analysis (Sharmila et al., 2016; Shakeel et al., 2015; Furuhashi & Weckwerth, 2013; Řezanka et al., 2003). Organic solvents such as chloroform, diethyl ether, hexane or methanol are used for the separation of lipid fractions, followed by methyl esterification catalysed using sulphuric acid or potassium hydroxide in methanol (Furuhashi & Weckwerth, 2013).

Several studies were reported on the characterisation of fatty acids and hydrocarbons in algae and cyanobacteria, via GC-MS. Fatty acids composition, namely, *n*-saturated, branched saturated, unsaturated, dioic and hydroxy were identified in the selected cyanobacteria (Řezanka et al., 2003). Majority of the fatty acids identified in GC-MS

were unsaturated and *n*-saturated, followed by branch saturated, and finally, dioic and hydroxy (Řezanka et al., 2003). In cold temperature, the viscosity of biofuels increases, affecting the performance of the liquid fuel and the engine, due to clogged filters. Saturated fatty acids with long aliphatic chain have a poor cold flow temperature, hence, operate less efficiently in cold temperature (Sharmila et al., 2016). Meanwhile, unsaturated fatty acids have lower oxidative stability and susceptible to oxidation, affecting biofuels operation with a rancid odour (Sharmila et al., 2016).

Besides, fatty acids and hydrocarbons such as 1,2-benzenedicarboxylic acid, mono(2-ethylhexyl) ester, palmitic acid, heptadecane and nonadecane identified in *Fischerella ambigua* (Devi & Mehta, 2016), while, cyclohexasiloxane, dodecamethyl- identified in *Gracilaria corticate* (Sharmila et al., 2016), are some of the main components of biofuels. Pradana et al. (2017) have reported that *Nannochlorpsis* spp. produced the highest algal oil yield, at 0.0346 g compared to *Arthrospira platensis* with the lowest yield, at 0.0121 g. Palmitic acid found in *Nannochlorpsis* spp. contributed to the high percentage of lipid oil, whereas, vice versa for oleic acid in *Arthrospira platensis*. *Nannochlorpsis* spp. is a good source of biofuels as it has the highest amount of saturated fatty acid, meanwhile, *Arthrospira platensis* is more suited as nutrition feeds (Pradana et al., 2017).

2.4.3 Raman Spectroscopy

The changes in the vibrational energy of a molecule are studied via Raman spectroscopy. When samples are subjected to monochromatic light, the major portion of the rays is transmitted, while, the remaining undergoes scattering, namely Rayleigh scattering and Raman scattering (Lin-Vien et al., 1991). In Rayleigh scattering, the excited electron in the virtual state returns to the initial vibrational state, when it loses its energy, and emits a photon with a frequency equal to the incident photon (Lin-Vien et al., 1991). On the contrary, in Raman scattering, the excited electron in the virtual state fall to a different vibrational state, and emits a photon with a frequency different to the incident photon (Lin-Vien et al., 1991). This frequency shift is known as the Raman shift.

For characterisation purposes, the Stokes line of the Raman band is preferred, as it exhibits a higher Raman intensity due to the absorbance of energy at a higher vibrational state (Lin-Vien et al., 1991). Similar to Raman spectroscopy, Infrared (IR) spectroscopy measures the vibrational frequency, but with different band intensities and excitation regions (Lin-Vien et al., 1991). Raman spectroscopy uses intense monochromatic incident rays, while, IR spectroscopy targets the IR region. Both IR and Raman analysis follows a correlation algorithm, whereby, a change in the dipole moment (antisymmetric vibrations) activates the IR spectrum, whereas, a change in the polarizability (symmetric vibrations) activates the Raman spectrum (Lin-Vien et al., 1991).

Raman spectroscopy is incorporated in various applications for the identification of chemical bonds and functional groups, characterisation of biomolecule components, surface analysis and equilibrium studies (Lin-Vien et al., 1991). Several studies were reported on the identification of photosynthetic pigments and biomolecule components in algae and cyanobacteria, each having its unique fingerprinting of Raman signals.

Jehlička et al. (2014) have reported the identification of photosynthetic pigments, namely chlorophylls, carotenoids, phycobilin, scytonemin and mycosporine-like amino acids, in algae and cyanobacteria. Different types of photosynthetic pigments provide a distinct and fingerprinting Raman band, enabling the characterisation of the pigments, either from pure cultures or environmental samples (Jehlička et al., 2014). The distinct Raman signatures enable an accurate differentiation of algae and cyanobacteria species.

Parab & Tomar (2012) have also reported the characterisation of biomolecule components such as haemoglobin, polysaccharides, glucosides, hydrocarbons and nucleic acids. It is observed that the Ferric bond of haemoglobin has a Raman peak at 440 cm^{-1}, 1502 cm^{-1} and 1374 cm^{-1}. Carbohydrates such as polysaccharides and glucosides have a Raman peak between 350–600 cm^{-1} and 479–483 cm^{-1}, respectively. Strong Raman peaks are observed in hydrocarbons in the range of 1650–1670 cm^{-1} and 2800–3000 cm^{-1}, and in nucleic acids between 600–800 cm^{-1}.

Moreover, the Raman band of carotenoids are detected at 1003 cm^{-1}, 1155 cm^{-1} and 1515 cm^{-1}, approximately (Baqué et al., 2018; Jehlička et al., 2014; Parab & Tomar, 2012; Pilát et al., 2012). The Raman signature of carotenoids was still intact and not affected, even after high dosage of gamma radiation, at 117 kilograys, was subjected to *Nostoc* spp. strain CCCryo 231-06 (Baqué et al., 2018). This suggested that the Raman spectroscopy is highly sensitive, as signals can be retrieved from damaged and deteriorated samples.

CHAPTER 3: METHODOLOGY

3.1 Sample Collection

Marine algae cultures; *C. calcitrans*, *I. galbana*, *Chlorella* spp., and *Tetraselmis* spp., were obtained from the International Institute of Aquaculture and Aquatic Sciences, Universiti Putra Malaysia. Meanwhile, freshwater cyanobacteria strains; *M. aeruginosa* (CCAP 1450/16) and *Nostoc* spp. (CCAP 1453/25), were purchased from the Culture Collection of Algae and Protozoa (CCAP), Scotland, United Kingdom. *C. calcitrans* and *I. galbana* are characterised as brown algae, *Chlorella* spp. and *Tetraselmis* spp. are characterised as green algae, and *M. aeruginosa* and *Nostoc* spp. are characterised as cyanobacteria, based on its phenotypic colour and photosynthetic pigments.

3.2 Propagation of Algae and Cyanobacteria

3.2.1 Conway and Blue-Green (BG11) Media

A seawater solution of 30 ppt salinity was prepared by adding 30 g of sea salt into 1 L of deionised water and sterilised at 15 psi (121 °C) for 15 min. Pre-sterilised stock solutions of Conway media comprising of macronutrients (1 ml), trace metals (0.5 ml) and vitamins (0.1 ml) were added into the seawater solution. Silicate and nitrate solutions, each at a volume of 1 ml, respectively, were added for the propagation of diatoms. The recipe for the preparation of Conway media stock solutions are shown in Appendix A.

Pre-sterilised stock solutions of Blue-green (BG11) media comprising of sodium nitrate ($NaNO_3$) (100 ml), other macronutrients (10 ml of each stock) and trace metals (1 ml) were added into 1 L of pre-sterilised deionised water. The pH was adjusted to 7.1 with 1 M of sodium hydroxide (NaOH) or hydrochloric acid (HCl). The recipe for the preparation of BG11 media stock solutions are shown in Appendix B.

3.2.2 Propagation and Subculture Conditions

An Erlenmeyer flask, 250 ml volume (Nalgene Thermo Fisher Scientific, US) was used as the culture flask in this study. Conway and BG11 media were freshly prepared before propagation. For the propagation of algae, 20 ml of existing algae stock was transferred into 30 ml of Conway media, with the use of a serological pipette (Nunc Thermo Fisher Scientific, US), in aseptic technique. For the propagation of the cyanobacteria, 5 ml of the strain was transferred into 50 ml of BG11 media, by using a serological pipette, in aseptic technique.

The cultures of algae and cyanobacteria were propagated in a cooling shaking incubator (N-BIOTEK NB-205LF, Korea), with culture conditions maintained at 24 °C and a rotational speed of 150 revolutions per minute (rpm), for aeration. A white fluorescent lamp with an intensity of 50 $\mu molm^{-2}s^{-1}$ was placed near the cultures, with 12 hr of photoperiods. A serial subculture was carried out once a week, in aseptic technique, and the cultures were harvested after successive subculture. The remaining cultures were continued for propagation and subcultured once a week until the next harvest.

3.2.3 Cell Density Measurement

Cell density or cell count of algae and cyanobacteria was determined using a counting chamber Neubauer Improved double net ruling (Marienfeld, Germany). Firstly, from 15 ml of *Nostoc* spp. culture, a volume of 20 µl was withdrawn and placed in an Eppendorf tube, followed by an equal volume of 0.4 % Trypan Blue solution (Thermo Fisher Scientific, US), and mixed gently. A 10 µl of the mixture was gently loaded in each counting chambers, by pipetting the mixture beneath the provided coverslip, following a capillary action.

Trypan Blue distinguishes between viable and dead cells by seeping into the cell membranes of the dead cells and stains it blue (Louis & Siegel, 2011). Only the corner squares and the middle square grids were taken into account. The cells were only counted when they were found within a square grid or on the right-hand or the bottom boundary line. The viable and dead cell counting was repeated with the remaining corner squares and the middle square, and with the rest of the algae and cyanobacteria samples. Cell density is determined by using the following calculation steps (Louis & Siegel, 2011).

$$Cell\ viability\ (\%) = \frac{Viable\ cell\ count}{Total\ cell\ count} \times 100\%$$

$$Average\ cell\ count = \frac{Viable\ cell\ count}{Total\ number\ of\ squares}$$

$$Dilution\ factor = \frac{Final\ volume}{Initial\ volume\ of\ cells}$$

$$Cell\ Density\ (cells/ml) = \frac{Average\ cell\ count \times Dilution\ factor}{Volume\ of\ squares\ (ml)}$$

3.3 Molecular Biomarkers

3.3.1 The p23SrV and 18Sr Biomarkers

3.3.1.1 DNA Extraction

The DNA of algae and cyanobacteria were extracted following the phenol-chloroform extraction protocol (Ausubel et al., 2003). The recipe for the preparation of reagents and buffers stock solutions are shown in Appendix C. A 15 ml of the cultures of algae and cyanobacteria were centrifuged (Eppendorf 5415R Centrifuge, Germany) at 10,000 rpm for 10 min. The pellet was transferred into a 2.0 ml microcentrifuge tube, centrifuged until a compact pellet was formed, and stored in -80 °C. Reagents such as Tris/EDTA (TE) buffer, sodium dodecyl sulfate (SDS) and cetyltrimethylammonium bromide/sodium chloride (CTAB/NaCl) solution were pre-heated at 65 °C beforehand.

The pellet was resuspended in 561 µl of TE buffer and homogenised by pipetting the mixture several times. A 30 µl of 10 % (w/v) SDS was added, which functions as a detergent for the lysis of the cell wall. In the next step, Proteinase K, RNase A and β-mercaptoethanol were added, each at a volume of 3 µl, respectively. Tannin and polyphenols which causes DNA degradation were removed by β-mercaptoethanol (Arruda et al., 2017). The total volume of the solution was 600 µl, and it was mixed well by inverting the tube several times before incubating in a water bath at 37 °C for 1 hr.

After the incubation period, 100 µl of 5 M NaCl was added, followed by the addition of 80 µl of CTAB/NaCl solution (10 % w/v CTAB in 0.7 M NaCl), and vortexed for 1 min. CTAB helps in the removal of denatured protein, cell wall debris, and polysaccharides. A concentration of NaCl below 0.5 M produces a precipitate of CTAB with nucleic acids (Ausubel et al., 2003). The solution was incubated at 65 °C for 10 min.

An equal volume of chloroform/isoamyl alcohol (24:1, v/v), approximately at 780 µl, was added into the solution, vortexed for 1 min, and centrifuged at 13,000 rpm for 5 min. The supernatant, excluding the white precipitate of CTAB, was transferred into a new 1.5 ml microcentrifuge tube. An equal volume of phenol/chloroform/isoamyl alcohol (25:24:1, v/v) was added, vortexed for 1 min, and centrifuged at 13,000 rpm for 5 min.

Subsequently, the supernatant was transferred into a new 1.5 ml microcentrifuge tube and 0.6 volume isopropyl alcohol was added to precipitate the nucleic acids. The tube was inverted gently until a white precipitate is visible. The samples were stored in -20 °C overnight if the precipitate is not visible. The samples were then centrifuged in a cool condition (at 4 °C), at 13,000 rpm for 20 min. The supernatant was carefully removed, and the pellet was washed with 700 µl of 70 % ethanol. Final centrifugation was carried out at 13,000 rpm for 5 min, and the supernatant was carefully removed. The pellet was air-dried for 30 min and dissolved in 100 µl of TE buffer.

The extracted DNA was quantitatively analysed using a Nanodrop spectrophotometer. The concentration of the nucleic acids (ng/µl) and the absorbance ratio at 260 nm and 280 nm was measured. For qualitative analysis, the genomic DNA was visualised under a UV transilluminator (VWR International, US) on a 1 % (w/v) agarose gel electrophoresis. The electrophoresis was run at a voltage of 100 V and a current of 200 mA for 40 min. Finally, the extracted DNA was stored in -20 °C freezer.

3.3.1.2 DNA Amplification

The p23SrV and 18Sr gene region were utilised in this study. The p23SrV biomarker is used for cyanobacteria and algae groups (Sherwood & Presting, 2007; Presting, 2006) while, the 18Sr biomarker is only used for the algae groups (Eman et al., 2016; Duong et al., 2015). The primer sequences are shown in Table 3.1.

Table 3.1: The primer sequences of p23SrV and 18Sr in 5' to 3' direction, with its respective melting temperature and amplicon size.

Primers	Primer Sequence (5' to 3' direction)	Melting Temperature (°C)	Amplicon Size (bp)
p23SrV_F1	5'-GGA CAG AAA GAC CCT ATG AA-3'	51.3	400
p23SrV_R1	5'-TCA GCC TGT TAT CCC TAG AG-3'	53.0	
18Sr_F1	5'-GCG GTA ATT CCA GCT CCA ATA GC-3'	58.2	500
18Sr_R1	5'-GAC CAT ACT CCC GGA ACC-3'	61.7	

A master mix was prepared which consisted of 5.0 µl of 5X colourless *GoTaq* reaction buffer (Promega, US), 1.5 µl of 25 mM magnesium chloride (Promega, US), 0.5 µl of 10 mM dNTP mix (Promega, US), 0.25 µl of *GoTaq* DNA polymerase (Promega, US), 1.0 µl of 10 mM of each primer (forward and reverse) and 1.2 µl of the DNA template. The master mix was brought to a final volume of 25 µl with the addition of nuclease-free water (Promega, US) and spun down for mixing. An extra volume of reagents (n+1) was added during the preparation of the master mix to avoid pipetting error.

A 25 µl of the master mix was transferred into a 0.2 ml PCR tube and spun down for mixing. PCR was performed in an Eppendorf Mastercycler EP gradient S thermal cycler (Eppendorf, Hamburg, Germany) using the cycling conditions, as shown in Table 3.2. The annealing temperature was set at 5 °C below the melting temperature of the primers.

Table 3.2: PCR cycling conditions for p23SrV and 18Sr biomarkers.

Biomarkers	PCR Cycling Condition
p23SrV	Initial denaturation: 94 °C, 2 min Denaturation: 94 °C, 20 sec Annealing: 46–50 °C, 30 sec Extension: 72 °C, 30 sec Final extension: 72 °C, 10 min 10 °C on hold 35 cycles
18Sr	Initial denaturation: 94 °C, 5 min Denaturation: 94 °C, 30 sec Annealing: 53–57 °C, 30 sec Extension: 72 °C, 2 min Final extension: 72 °C, 10 min 10 °C on hold 35 cycles

To assess the quality of the PCR product, a 2 % (w/v) agarose gel was prepared and submerged into the electrophoresis chamber that was filled with 1 × Tris base/Acetic acid/EDTA (TAE) buffer. The PCR product was mixed with the 5X green *GoTaq* loading buffer (Promega, US) in a ratio of 4:1, and loaded gently into the wells of the submerged gel. A 3 µl of 100 base pair (bp) DNA ladder (TransGen Biotech, China) was loaded as a reference ladder. The electrophoresis was run at a voltage of 80 V and a current of 180 mA for 30 min. Lastly, the gel was visualized under a UV transilluminator, and the PCR products with intact bands were sent for sequencing.

3.3.1.3 Phylogenetic Tree and Median-Joining Network Analysis

The forward and the reverse sequences were inserted in MEGA7 alignment explorer. The reverse sequences were reverse complemented to ensure both forward and reverse sequences are in the same direction. The sequences were next aligned by ClustalW and edited. The edited sequences were exported to MEGA (.meg) and FASTA (.fas) file. Using the .meg file, Neighbor-Joining tree was constructed based on the Kimura 2-parameter substitution model and a bootstrap replicate of 1000. Pairwise distances were also computed in MEGA7. A nucleotide BLAST search was performed to compare and identify the library sequences that resembled the query sequences.

The generation of haplotype data was accomplished via DNA sequence polymorphism (DnaSP 5.10) software (Rozas, 2009). The saved .meg or .fas file was opened in DnaSP 5.10 and the genetic code was assigned. The 'defining the sequence set' was selected for the grouping of populations. For the generation of haplotype data, the parameter 'Arlequin haplotype list' was chosen and saved as .hap file and .arp file. The generated haplotype data was exported to Roehl file (.rdf) for the network analysis.

Network 5.0.1.0 software was used to generate the median-joining haplotype network (Forster, 2015). In Network 5.0, 'median-joining' was selected, and the .rdf file was chosen to calculate the network. The .out file was saved. In a new window, the .out file was opened, and a network diagram was created. The diagram was edited by dragging the median vector for better graphical representation and saved in a .fdi format.

3.3.2 mcy Gene Cluster

A set of seven primers were utilised to validate the presence of the mcy gene cluster, which encodes the biosynthesis of microcystin (Table 3.3), as reported by Ouahid et al. (2005). The mcyA amplifies the NMT domain, the mcyB and mcyC amplify the adenylation domain, the mcyD amplify the acyl carrier protein and the β-ketoacyl synthase domain, the mcyE amplifies the glutamate-1-semialdehyde aminotransferase domain, and the mcyG amplifies the C-methyltransferase domain.

Table 3.3: The primer sequences of the mcy gene cluster in 5' to 3' direction, with its respective melting temperature and amplicon size (Ouahid et al., 2005).

Gene	Primers	Primer Sequence (5' to 3' direction)	Melting Temperature (°C)	Amplicon Size (bp)
mcyA	MSF	5'-ATC CAG TTG AGC AAG C-3'	55.9	1300
	MSR	5'-TGC AGA TAA CTC CGC AGT TG-3'	55.2	
mcyB	2156-F	5'-ATC ACT TCA ATC TAA CGA CT-3'	47.2	955
	3111-R	5'-AGT TGC TGT AAG AAA-3'	47.9	
mcyC	PSCF1	5'-GCA ACA TCC CAA GAG CAA AG-3'	54.6	674
	PSCR1	5'-CCG ACA TCA CAA AGG C-3'	54.5	
$mcyD_1$	PKDF1	5'-GAC GCT CAA ATG AAA C-3'	48.7	647
	PKDR1	5'-GCA ACC GAT AAA AAC TCC C-3'	51.2	
$mcyD_2$	PKDF2	5'-AGT TAT TCT CCT CAA GCC-3'	47.9	859
	PKDR2	5'-CAT TCG TTC CAC TAA ATC C-3'	47.6	
mcyE	PKEF1	5'-CGC AAA CCC GAT TTA CAG-3'	51.4	755
	PKER1	5'-CCC CTA CCA TCT TCA TCT TC-3'	52.0	
mcyG	PKGF1	5'-ACT CTC AAG TTA TCC CTC-3'	52.9	425
	PKGR1	5'-AAT CGC TAA AAC GCC ACC-3'	53.3	

A PCR master mix was prepared which consisted of 12.5 µl of 2 × Power Taq MasterMix (BioTeke, China), 1.25 µl of 10 mM of each primer (forward and reverse) and 1.25 µl of the DNA template. Nuclease-free water was added for a final volume of 25 µl. The master mix was transferred into a 0.2 ml PCR tube and spun down for mixing. PCR was performed in the thermal cycler using the cycling conditions, as shown in Table 3.4. The annealing temperature was set at 5 °C below the melting temperature of the primers.

Table 3.4: PCR cycling conditions for the mcy gene cluster primers.

Primers	PCR Cycling Condition	Annealing Temperature (°C)
mcyA	Initial denaturation: 95 °C, 5 min Denaturation: 95 °C, 1 min Annealing: 44–51 °C, 30 sec Extension: 72 °C, 1 min Final extension: 72 °C, 10 min 10 °C on hold 35 cycles	51
mcyB		45
mcyC		50
$mcyD_1$		44
$mcyD_2$		44
mcyE		48
mcyG		49

To assess the quality of the PCR product, a 2 % (w/v) agarose gel was prepared and submerged into the electrophoresis chamber filled with 1 × TAE buffer. A 5 µl of the PCR product was loaded gently into the wells of the submerged gel. A 3 µl of 100 bp DNA ladder was loaded as a reference ladder. The electrophoresis was run at a voltage of 80 V and a current of 180 mA for 30 min. Lastly, the gel was visualized under a UV transilluminator, and the PCR products with intact bands were sent for sequencing.

The PCR products with multiple bands were purified using the Wizard SV Gel and PCR Clean-Up System (Promega, US). In a 1.5 ml microcentrifuge tube, 10 µl of membrane binding solution was added for every 10 mg of the gel slice, vortexed, and incubated at 65 °C. The dissolved gel mixture was transferred into a minicolumn with a collection tube and incubated at room temperature for 1 min. The minicolumn was centrifuged at 16,000 × g for 1 min and the flow-through was discarded.

Then, 700 µl of membrane wash solution was added and centrifuged at 16,000 × g for 1 min. Another 500 µl of the membrane solution was added and centrifuged at 16,000 × g for 5 min. The minicolumn was centrifuged once more at 16,000 × g for 1 min. The flow-through was discarded. The minicolumn was next transferred into a new 1.5 ml microcentrifuge tube, and 50 µl of nuclease-free water was added. The tube was incubated at room temperature for 1 min, followed by centrifugation at 16,000 × g for 1 min. Lastly, the minicolumn was discarded and the purified DNA was stored at -20 °C.

Subsequently, a PCR master mix was prepared which consisted of 12.5 µl of 2 × Power Taq MasterMix, 1.25 µl of 10 mM of each primer (forward and reverse) and 1.25 µl of the purified DNA template. PCR was performed in the thermal cycler using the cycling conditions as shown in Table 3.4. A 2 % (w/v) agarose gel was prepared to assess the quality of the PCR product. The electrophoresis was run at a voltage of 80 V and a current of 180 mA for 30 min. The gel was visualized and the PCR products with intact bands were sent for sequencing. A protein BLAST search was performed to compare and identify the library sequences that resembled the query sequences.

3.4 GC-MS

3.4.1 Solvent Extraction

Solvent extraction was carried out to separate the organic phase of algae and cyanobacteria from the inorganic substances. The solvent extraction was carried out in a fume hood using a separatory funnel (Nalgene Thermo Fisher Scientific, US), in small extraction volumes, for an efficient separation process (Adams et al., 1975). Hexane (HPLC grade Sigma-Aldrich, US), a non-polar organic solvent, was used as the organic phase (Pradana et al., 2017; Samori et al., 2010).

The hexane was transferred into the separatory funnel using a glass funnel. A volume of 15 ml of each culture of algae and cyanobacteria were harvested. A small batch of volumes, about 5 ml, was transferred into the same separatory funnel. The separatory funnel was shaken in a horizontal position vigorously, followed by venting. This process was repeated for several times. Then, the separatory funnel was swirled to allow the two layers to settle down quickly and eventually were separated into two layers.

The bottom layer was drained out and discarded, as the organic phase is less dense than the aqueous or inorganic phase. The entire process was repeated with the remaining of the harvested cultures. The organic phase was later collected in a clean Erlenmeyer flask. A drying agent, anhydrous sodium sulphate (Sigma-Aldrich, US) was added to absorb excess moisture. Sodium sulphate was added until a clear transparent solution with the solids of the drying agent was observed. The solution was filtered over a nylon membrane filter (0.45 μm pore size) and transferred into a vial for the GC-MS analysis.

3.4.2 GC-MS Analysis

The GC-MS analysis was performed using the Agilent 6890N Network GC system, equipped with Agilent J&W DB-5 capillary column (30.00 m length × 0.24 mm internal diameter × 1.00 μm film thickness) and Agilent 5973 Network Mass Selective Detector. The mobile phase is the helium and the stationary phase is the capillary column. The sample (1 μl) was injected into the injection port using a syringe (Hamilton, US), which was thrust into the column with the help of the carrier gas (Adesalu et al., 2016). The injector temperature was at 260 °C with a split ratio of 10:1. The flow rate of the helium was at 1 ml/min. The oven temperature was pre-set at 40 °C for 5 min, increased from a rate of 10 °C/min, to a final temperature at 260 °C for 5 min.

The GC column allows the separation of compounds based on its volatility and polarity (Adesalu et al., 2016). Retention time is the time taken for a compound to pass through the column, and a chromatogram peak was detected once the compound was eluted out (Adesalu et al., 2016). The area of the peak represents the amount or the concentration of the compound. The mass selective detector works at 285 °C, with an ionisation voltage of 70 eV, and an electron mass scan from 30 to 700 mass-to-charge ratio (m/z), at 0.9 scan/s. The solvent delay was at 3 min. The total run time per sample was 30 min. The mass spectra of the eluted compounds were identified using the NIST98.L library match.

3.5 Raman Spectroscopy

3.5.1 Sample Preparation

A sterilised microscope glass slides were used as the base of a thin film of algae and cyanobacteria. The glass slides (Sail Brand, China) were sterilised following the cleaning protocol of quartz substrate (Sundholm, 2009; Cras et al., 1999).

The glass slides were soaked in dishwashing soap and immersed in an ultrasonic bath (Thermo-6D Thermo-Line, Australia) for 15 min. The glass slides were rinsed in deionised water, acetone, and isopropyl alcohol, for 5 min, respectively, and a final rinse in deionised water. A nitrogen gas gun was used to blow-dry the glass slides to remove water, dust and other residues.

A volume of 5 ml of each culture of algae and cyanobacteria were harvested and centrifuged at 10,000 rpm for 10 min. The pellet was washed twice with deionised water. The pellet was evenly layered on the sterilised glass slides and dried overnight. The dried thin films then proceeded for the spectral acquisition of Raman spectroscopy.

3.5.2 Spectral Acquisition

Renishaw In Via Raman microscope was operated following the manufacturer's protocol (Tan, 2010). The Renishaw's Raman system and the desired laser (514 nm laser was used in this study) were switched on for operation. In Renishaw's Windows-based Raman Environment (WiRE) software, the 'Reference All Motors' was selected for the initialisation check of the microscope motors, and the system was warmed up for 20 min.

For calibration, the silicon (Si) wafer reference was placed on the microscope stage using forceps and secured with the stage clip. The surface of the Si wafer was examined with the 5X objective lens. The 'Internal Si Reference Measurement (514 nm)' was selected, followed by the selection of 'Measurement>Run', to collect the Raman spectrum of Si. The peak position was checked. The system was calibrated by selecting 'Tools>Calibration>Quick Calibration' if the frequency is not within 520–521 cm^{-1}.

Following calibration, the sample (a thin film of algae or cyanobacteria) was placed on the microscope stage. The surface of the sample was examined with the 20X or 50X objective lens. Using a joystick, the region of interest was positioned to the centre of the crosshair of the laser. The 'Measurement>New>Spectral Acquisition' was selected and the 'spectral acquisition setup' panel was modified. Then, the 'Measurement>Run' was selected to collect the Raman spectra of the samples, and the spectra were saved.

The spectra data were also optimised for baseline subtraction, by selecting 'Processing>Subtract Baseline', followed by the selection of 'Properties>Cubic Spline Interpolation'. Finally, the 'Analysis>Peak Pick' was selected for peak analysis.

3.5.3 Spectral Analysis

The Bio-Rad KnowItAll Informatics System software was utilised for the spectral analysis. From the 'Settings' tab, the search method was selected to 'correlation'. The 'ID Expert' icon was then selected from the 'Data' panel. The 'New Search' was selected and the raw data of the Raman spectrum was uploaded. In the 'Technique Parameters' window panel, the data type was changed to 'Raman'. The search status will be loaded, showing a panel mixture of component results, peak results and functional groups.

The 'Optimised Corrections' was enabled from the 'Settings' tab, and the 'Noise Fix' was selected. Both selections increased the hit score of the identified components. Lastly, 'Create Report' was selected, whereby, a report of the desired components that has the best match with the reference spectra was generated. Additionally, a detailed search on the functional group analysis was determined from the 'Spectral Analysis' panel. The 'Browse a Functional Group' was selected from the 'Analyze' tab, and the desired functional group type was selected. The query spectrum (unknown spectrum) corresponded with the closest match of the reference functional group.

ID expert was able to measure the query spectrum and performed an algorithm match, to compare the query spectrum to the available database of Raman. The results were sorted with the closest match (hit score) of the reference spectra, at the top of the list, and the quality of the matches was assessed.

CHAPTER 4: RESULTS

4.1 Cell Density Measurement

The cell density of the selected algae and cyanobacteria was calculated using a counting chamber Neubauer Improved, with a dilution factor of 2 (Table 4.1). All the cells were 100% viable. The calculation steps of the cell density measurement are shown in Appendix D.

Table 4.1: Cell density and cell viability of the selected algae and cyanobacteria.

Species	Cell Density (cells/ml) ($\times 10^3$)	Cell Viability (%)
C. calcitrans	100	100
I. galbana	108	
Chlorella spp.	114	
Tetraselmis spp.	118	
M. aeruginosa	188	
Nostoc spp.	190	

4.2 Molecular Biomarkers

4.2.1 The p23SrV and 18Sr Biomarkers

4.2.1.1 DNA Extraction

Quantitative analysis using a Nanodrop spectrophotometer determined the concentration and purity of the extracted nucleic acids. The A260/A280 and A260/A230 ratio were obtained at 1.89 to 2.09 and 1.99 to 2.23, respectively (Table 4.2). Both values indicated a good purity of the extracted DNA. The genomic DNA was visualised on a 1% agarose gel electrophoresis and intact bands with faint smearing were observed for all the samples, as shown in Figure 4.1.

Table 4.2: Concentration and purity of the extracted nucleic acids from the selected algae and cyanobacteria.

Species	Nucleic Acid Concentration (ng/µl)	A260/A280	A260/A230
C. calcitrans	105.7	1.99	1.99
I. galbana	120.2	2.06	2.11
Chlorella spp.	99.3	2.09	2.03
Tetraselmis spp.	133.7	2.05	2.23
M. aeruginosa	121.1	1.89	2.20
Nostoc spp.	129.5	2.02	2.16

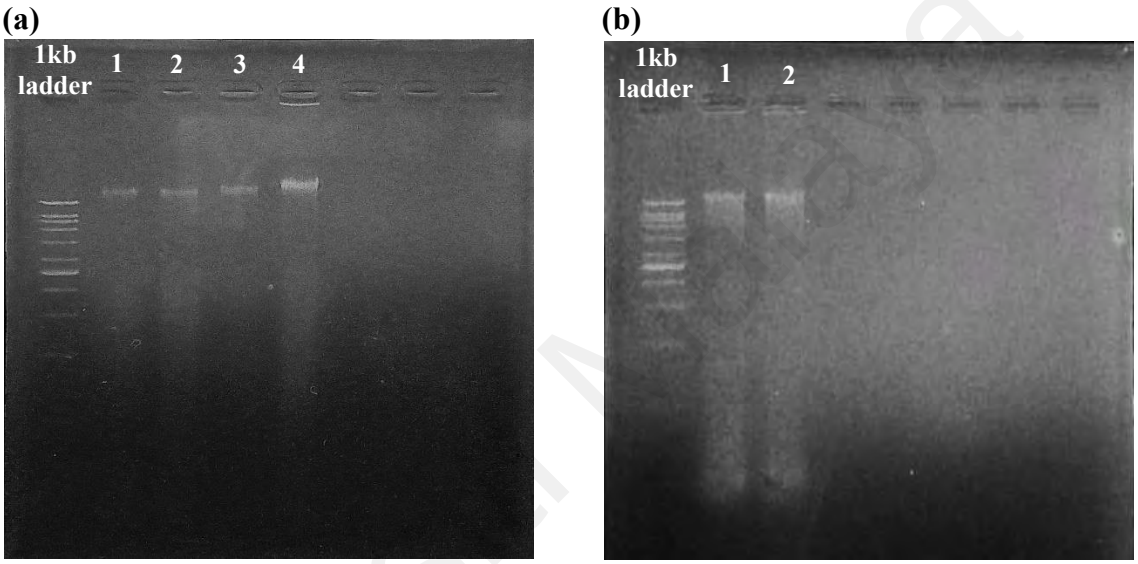

Figure 4.1: Gel image of genomic DNA of (a) algae (Lane 1 to 4: *C. calcitrans*, *I. galbana*, *Chlorella* spp. and *Tetraselmis* spp., respectively); and (b) cyanobacteria (Lane 1 to 2: *M. aeruginosa* and *Nostoc* spp., respectively)

4.2.1.2 DNA Amplification

The DNA of algae and cyanobacteria were successfully amplified, and the PCR products were visualised on a 2% agarose gel electrophoresis. With successful amplification using the p23SrV biomarker, thick intact bands at 400 bp amplicon size were observed in the PCR product of algae and cyanobacteria, annealed at 46–50°C (Figure 4.2). By using the 18Sr biomarker, thick intact bands at 500 bp amplicon size were observed in the PCR product of algae, annealed at 53–57°C (Figure 4.3).

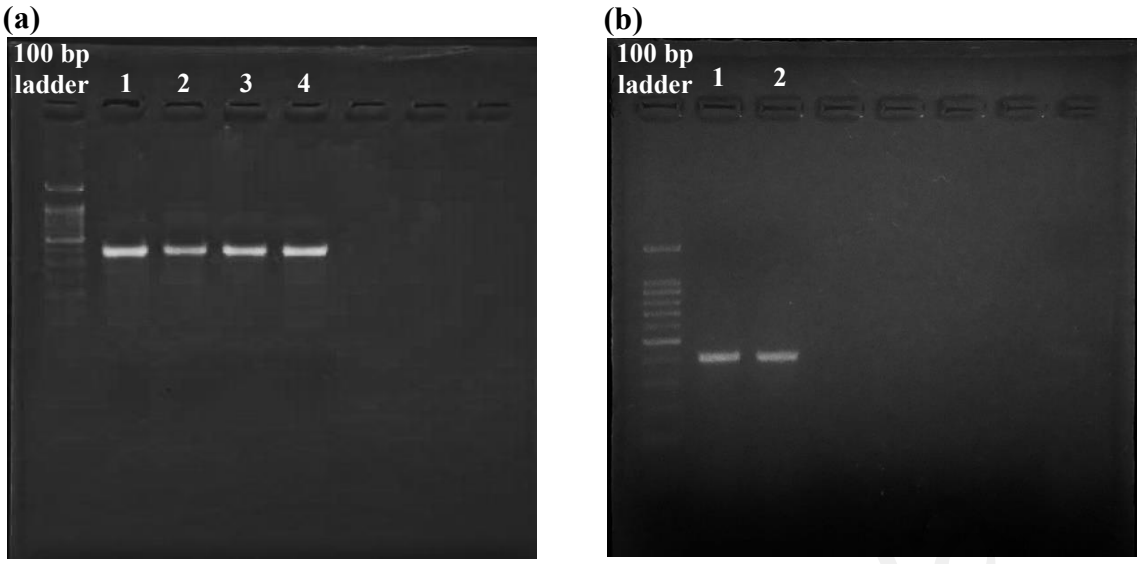

Figure 4.2: Gel image of p23SrV biomarker amplified in (a) algae (Lane 1 to 4: *C. calcitrans*, *I. galbana*, *Chlorella* spp. and *Tetraselmis* spp., respectively); and (b) cyanobacteria (Lane 1 to 2: *M. aeruginosa* and *Nostoc* spp., respectively)

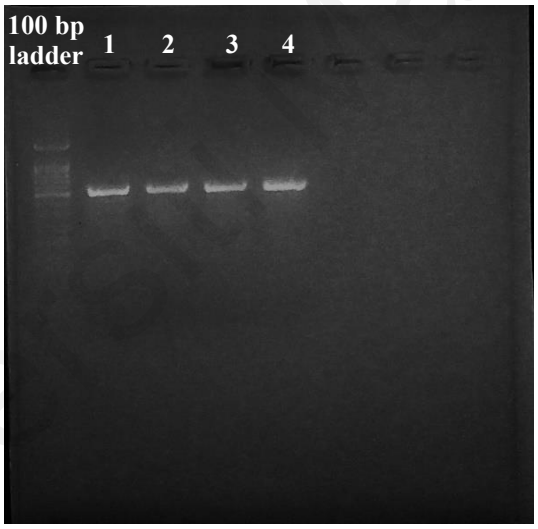

Figure 4.3: Gel image of 18Sr biomarker amplified in algae (Lane 1 to 4: *C. calcitrans*, *I. galbana*, *Chlorella* spp. and *Tetraselmis* spp., respectively)

4.2.1.3 Phylogenetic Tree and Median-Joining Network Analysis of p23SrV

The p23SrV sequences of algae and cyanobacteria (Appendix E) and the selected sequences retrieved from the NCBI GenBank database were aligned using ClustalW. The accession number of the retrieved sequences are shown in Appendix F. The construction of the Neighbor-Joining tree represented the evolutionary relationships of the investigated algae and cyanobacteria (Figure 4.4). *Gloeobcter violaceus* was selected as the outgroup species to root the phylogenetic tree.

The Neighbor-Joining tree shows a clear separation of brown algae, red algae, green algae and cyanobacteria clades, similar to Sherwood & Presting (2007) and Presting (2006). There were two clades observed from the Neighbor-Joining tree, which were the algae and the cyanobacteria clade. The subclades of algae were the red algae, brown algae and green algae. All the studied species were grouped in its expected clades; with *C. calcitrans* and I*. galbana* as brown algae, *Chlorella* spp. and *Tetraselmis* spp. as green algae, and *M. aeruginosa* and *Nostoc* spp. as cyanobacteria.

The bootstrap support of brown algae, green algae and cyanobacteria clades were at 76%, 92% and 83%, respectively. The higher percentage of bootstrap support indicated the close relationship between the species. The green algae, *Chlorella* spp. and *Tetraselmis* spp. were closely related, and the closest neighbours of the brown algae, *C. calcitrans* and *I. galbana*. The algae groups were distantly related to the cyanobacteria, *M. aeruginosa* and *Nostoc* spp. Moreover, *Chlorella* spp. was conspecific to *Parachlorella* spp., *Tetraselmis* spp. was closely related to *Tetraselmis chuii*, and *Nostoc* spp. was conspecific to *Nostoc commune*.

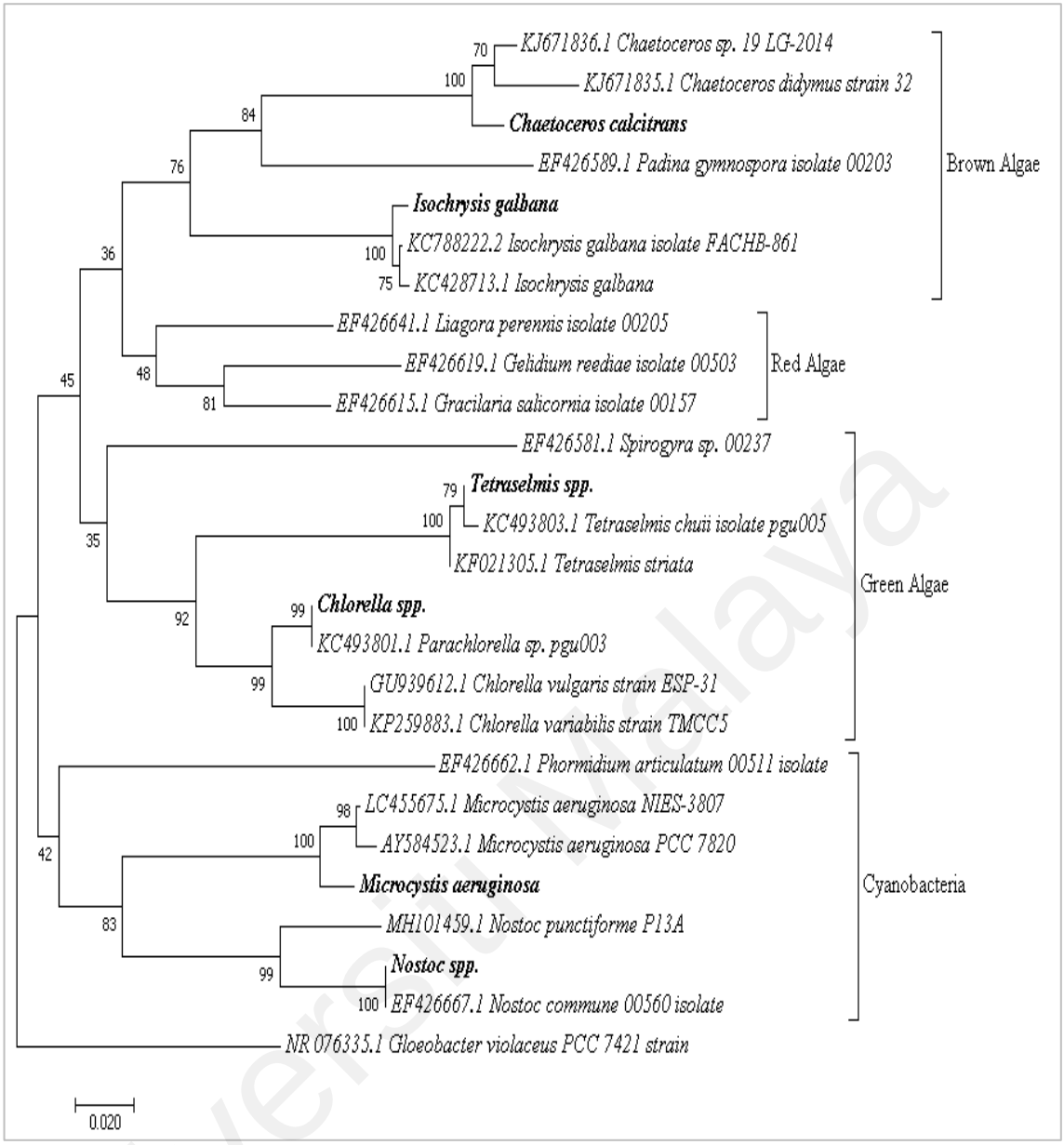

Figure 4.4: Neighbor-Joining tree of the selected algae and cyanobacteria based on the p23SrV sequence data. The studied species are shown in bold

Table 4.3: Pairwise distances of the selected algae and cyanobacteria.

	Pairwise Distances					
C. calcitrans						
I. galbana	0.211					
Chlorella spp.	0.260	0.226				
Tetraselmis spp.	0.259	0.257	0.126			
M. aeruginosa	0.251	0.230	0.197	0.285		
Nostoc spp.	0.267	0.226	0.216	0.280	0.174	
G. violaceus (Outgroup)	0.269	0.207	0.231	0.293	0.212	0.213

Pairwise distance is the measurement of evolutionary distances or divergences between each pair of species, and it was computed in a matrix table, as shown in Table 4.3. The pairwise distance between *C. calcitrans* and *I. galbana*; *Chlorella* spp. and *Tetraselmis* spp.; and *M. aeruginosa* and *Nostoc* spp.; were 0.211, 0.126 and 0.174, respectively. A total of 321 bp of partial sequences of p23SrV were amplified in algae and cyanobacteria. In brown algae, 260 characters were in the conserved sites and 60 characters were in the variable sites. In green algae, 284 characters were in the conserved sites and 37 characters were in the variable sites. Whereas, in cyanobacteria, 266 characters were in the conserved sites and 54 characters were in the variable sites.

The median-joining haplotype network was constructed to study the relationship of the population haplotype (Figure 4.5). Four distinct networks were observed between the red algae haplogroup (H_8 to H_10), the brown algae haplogroup (H_1 to H_7), the green algae haplogroup (H_11 to H_18), and the cyanobacteria haplogroup (H_19 to H_25). In each haplogroup, the closely related haplotypes were clustered; for instance, H_1, H_2 and H_3 were from the Genus Chaetoceros. The number of median vectors (black nodes) was higher for the brown algae haplogroup compared to the green algae haplogroup. The parsimony-informative sites of these haplotypes are shown in Appendix G.

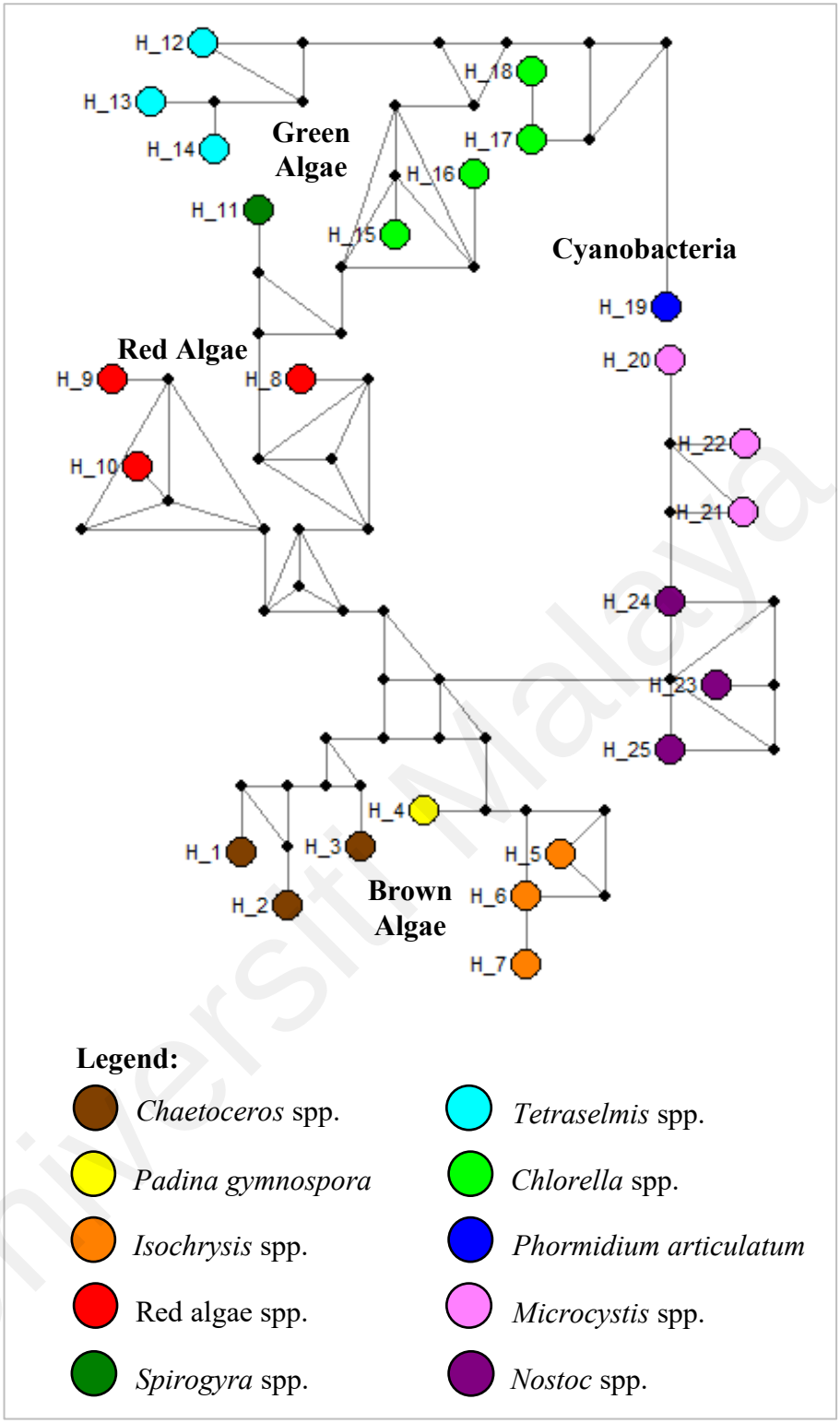

Figure 4.5: Median-joining network of the selected algae and cyanobacteria haplotypes

4.2.1.4 Phylogenetic Tree and Median-Joining Network Analysis of 18Sr

The 18Sr sequences of algae (Appendix E) were aligned using ClustalW. The construction of the Neighbor-Joining tree represented the evolutionary relationships of the investigated algae (Figure 4.6). *Euglena gracilis* was selected as the outgroup species to root the phylogenetic tree. There were two clades observed from the Neighbor-Joining tree, which were *C. calcitrans* and a clade comprising of green algae and *I. galbana*.

The bootstrap support of green algae and *I. galbana* were at 95% and 59%, respectively. The higher percentage of bootstrap support indicated the close relationship between the species. The green algae, *Chlorella* spp. and *Tetraselmis* spp. were closely related, and the closest neighbours of the haptophyte, *I. galbana*. The diatom, *C. calcitrans* were distantly related to *I. galbana*.

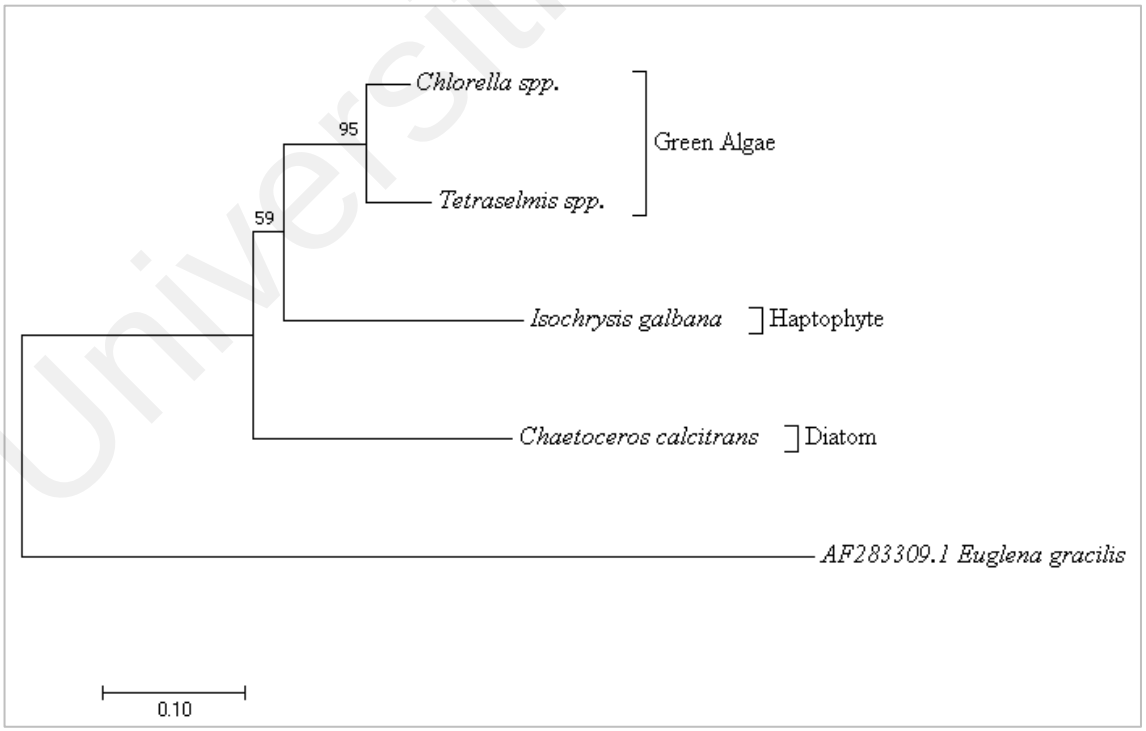

Figure 4.6: Neighbor-Joining tree of the selected algae based on the 18Sr sequence data

The pairwise distance was computed in a matrix table, as shown in Table 4.4. The pairwise distance between *C. calcitrans* and *I. galbana*; and *Chlorella* spp. and *Tetraselmis* spp.; were 0.376 and 0.075, respectively. A total of 504 bp of partial sequences of 18Sr were amplified in the algae groups. In brown algae, 354 characters were in the conserved sites and 146 characters were in the variable sites. In green algae, 467 characters were in the conserved sites and 37 characters were in the variable sites.

Table 4.4: Pairwise distances of the selected algae groups.

	Pairwise Distances			
C. calcitrans				
I. galbana	0.376			
Chlorella spp.	0.280	0.233		
Tetraselmis spp.	0.305	0.294	0.075	
E. gracilis (Outgroup)	0.898	0.900	0.860	0.821

The median-joining haplotype network was constructed to study the relationship of the population haplotype (Figure 4.7). Two distinct networks were observed between the brown algae haplogroup (H_1 and H_2) and the green algae haplogroup (H_3 and H_4), with its respective rate of mutation. The number of mutations was higher for the brown algae haplogroup compared to the green algae haplogroup. The parsimony-informative sites of these haplotypes are shown in Appendix G.

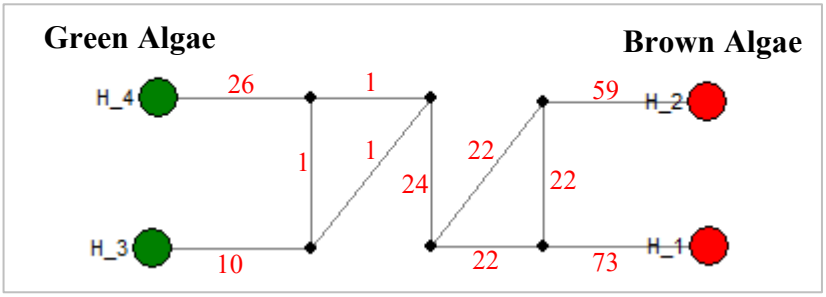

Figure 4.7: Median-joining network of the selected algae haplotypes

4.2.2 mcy Gene Cluster

The mcy gene cluster was not amplified in *M. aeruginosa* and *Nostoc* spp. The mcy gene cluster consisting of mcyA–C of the NRPS domain, mcyD of the PKS domain, and mcy E and G of the NRPS-PKS hybrid domain, activates the biosynthesis of microcystin during amplification. However, in *M. aeruginosa* and *Nostoc* spp., bands were absent at the expected amplicon size. Non-specific bands at different amplicon size were observed. The protein BLAST search of the sequences of *M. aeruginosa* and *Nostoc* spp., encoded for NADPH-quinone oxidoreductase, ribonucleoside-diphosphate reductase and biotin co-factor. Hence, the biosynthesis of microcystin was inactivated or not expressed. Both of the cyanobacteria species may have lost the ability to biosynthesise microcystin, producing non-toxic strains.

4.3 GC-MS

The biosynthesis of organic compounds in the selected algae and cyanobacteria were analysed using the GC-MS. The organic compounds; namely alkane, alkyne, alcohol, phenol, polycyclic hydrocarbon, aromatic ketone and siloxane, were detected in *C. calcitrans*, *Tetraselmis* spp., *M. aeruginosa* and *Nostoc* spp. These compounds are incorporated in biofuels production, cosmetics, industrial lubricants and paint coatings.

The GC-MS chromatogram represented the organic compounds detected in algae (*C. calcitrans* and *Tetraselmis* spp.) (Figure 4.8), and cyanobacteria (*M. aeruginosa* and *Nostoc* spp.) (Figure 4.9), with its respective retention time. The organic compounds with higher volatility pass through the GC column faster and resulted in shorter retention time (Table 4.5). Table 4.5 also shows the total amount or the concentration of the organic compounds which is proportional to the area of the peak.

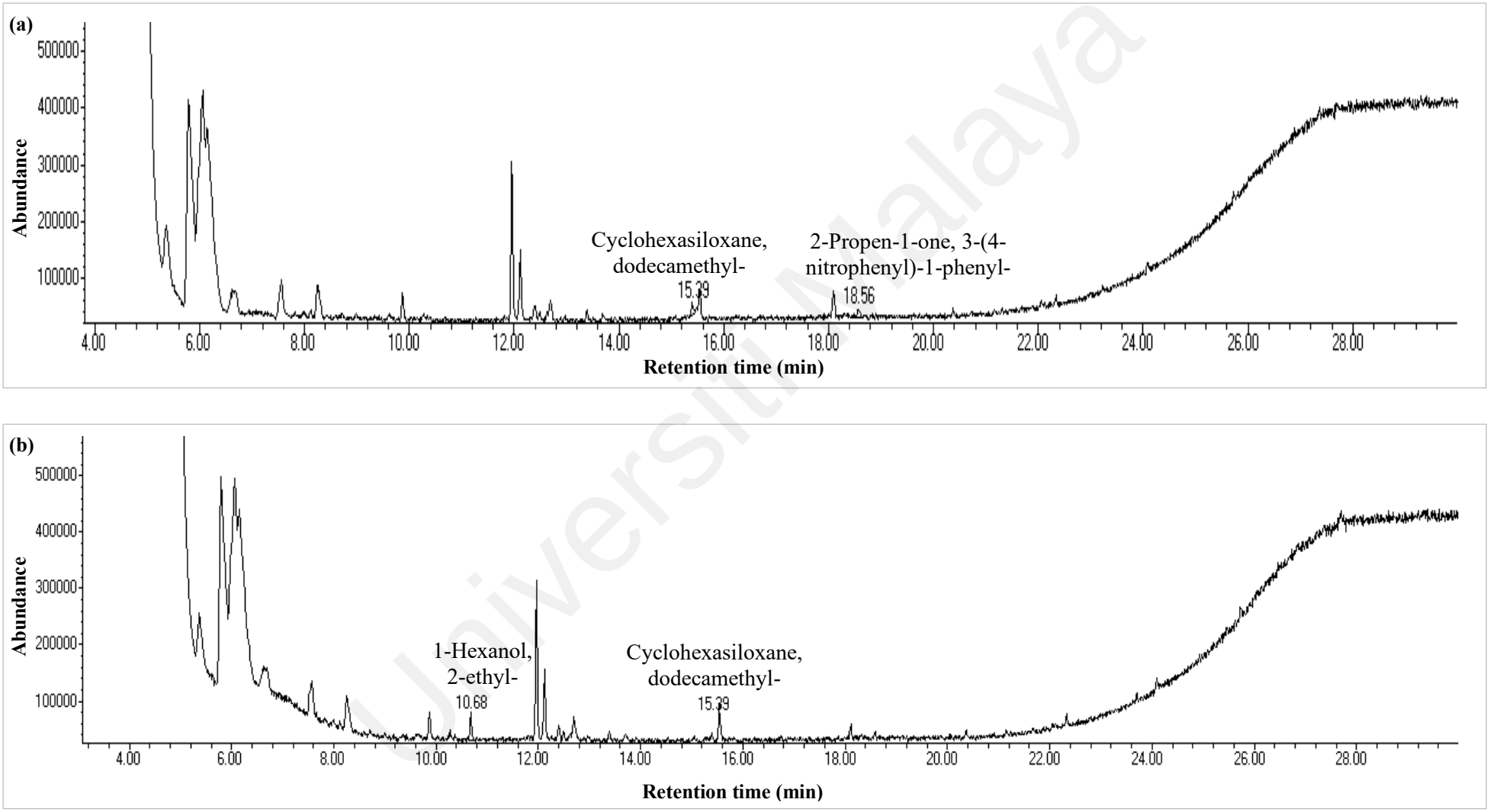

Figure 4.8: GC-MS chromatogram of organic compounds detected in (a) *C. calcitrans* and (b) *Tetraselmis* spp., with its respective retention time

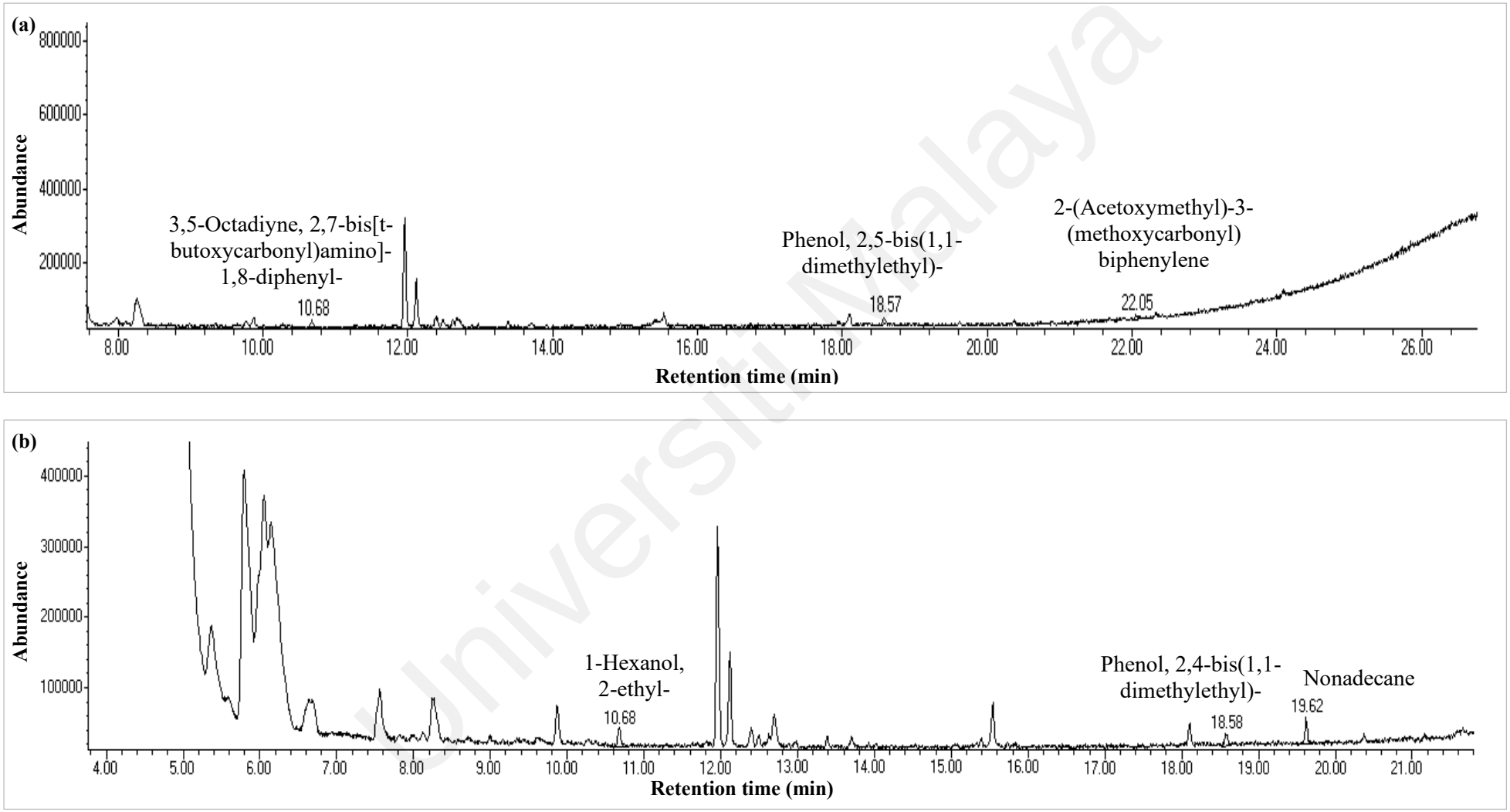

Figure 4.9: GC-MS chromatogram of organic compounds detected in (a) *M. aeruginosa* and (b) *Nostoc* spp., with its respective retention time

Table 4.5: The different types of organic compounds eluted, with its respective retention time, peak area, total amount and boiling point.

Samples Tested	Types of Organic Compounds Eluted	Retention Time (min)	Peak Area	Total Amount (%)	Boiling Point (°C)
C. calcitrans	Cyclohexasiloxane, dodecamethyl-	15.39	561548	47.30	245.00
	2-Propen-1-one, 3-(4-nitrophenyl)-1-phenyl-	18.56	625758	52.70	399.20
Tetraselmis spp.	1-Hexanol, 2-ethyl-	10.68	1151053	42.43	185.00
	Cyclohexasiloxane, dodecamethyl-	15.39	1561548	57.57	245.00
M. aeruginosa	3,5-Octadiyne, 2,7-bis[t-butoxycarbonyl)amino]-1,8-diphenyl-	10.68	420419	34.32	663.70
	Phenol, 2,5-bis(1,1-dimethylethyl)-	18.57	456878	37.29	283.40
	2-(Acetoxymethyl)-3-(methoxycarbonyl) biphenylene	22.05	347820	28.39	430.30
Nostoc spp.	1-Hexanol, 2-ethyl-	10.68	805904	37.56	185.00
	Phenol, 2,4-bis(1,1-dimethylethyl)-	18.58	502098	23.41	263.50
	Nonadecane	19.62	837414	39.03	330.00

The organic compounds that are highly volatile or vaporised easily have lower boiling points, therefore, eluted earlier from the GC column (Adesalu et al., 2016). The most volatile compound was 1-hexanol, 2-ethyl-, compared to 3,5-octadiyne, 2,7-bis[t-butoxycarbonyl)amino]-1,8-diphenyl-, as the least volatile (Table 4.5). Conversely, 3,5-octadiyne, 2,7-bis[t-butoxycarbonyl)amino]-1,8-diphenyl-, as the most polar compound, was eluted first in *M. aeruginosa*, although with the lowest volatility.

The mass spectra using the NIST98.L library match (Appendix H) represented the abundance of the ion fragments over its relative molecular mass or m/z. The largest value of the m/z represented the molecular ion, and the other lower values of the m/z represented the relative mass of the ion fragments of the compounds.

4.4 Raman Spectroscopy

A thin film of the selected algae and cyanobacteria were analysed in the Renishaw's Raman spectroscopy to determine the vibrational properties that occur during the Raman scattering. The in-built Renishaw's WiRE software was used in the spectral acquisition analysis. The obtained Raman spectra were further optimised by using the baseline subtraction (background noise elimination) and the peak analysis function. The optimised Raman spectra are shown in Appendix I.

The ID expert panel of the Bio-Rad KnowItAll Informatics System software was able to perform the spectral search of the query spectrum (unknown spectrum), and execute a query match or a hit score with the closest reference spectra, from the available database. The top hit of the query corresponded with saffron, with a hit score of 84–94%. Whereas, the second hit on the list belongs to carotene, with a hit score of 72–84%. Saffron and carotene were the two prominent compounds found in all the analysed samples. The Raman spectra of saffron and carotene are shown in Figures 4.10 and 4.11, respectively.

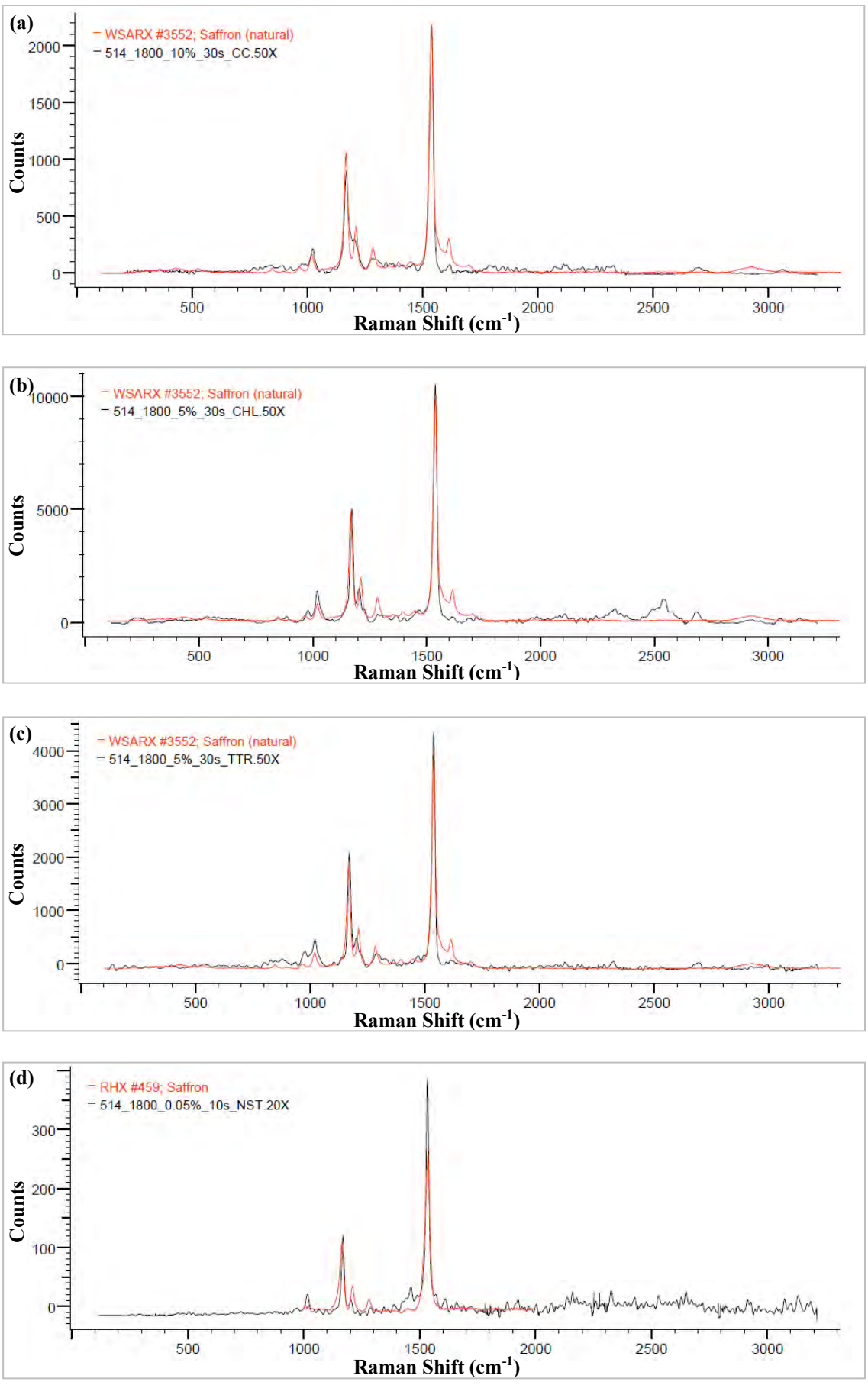

Figure 4.10: Raman spectra of saffron in (a) *C. calcitrans* (94% match); (b) *Chlorella* spp. (91% match); (c) *Tetraselmis* spp. (91% match); and (d) *Nostoc* spp. (84% match)

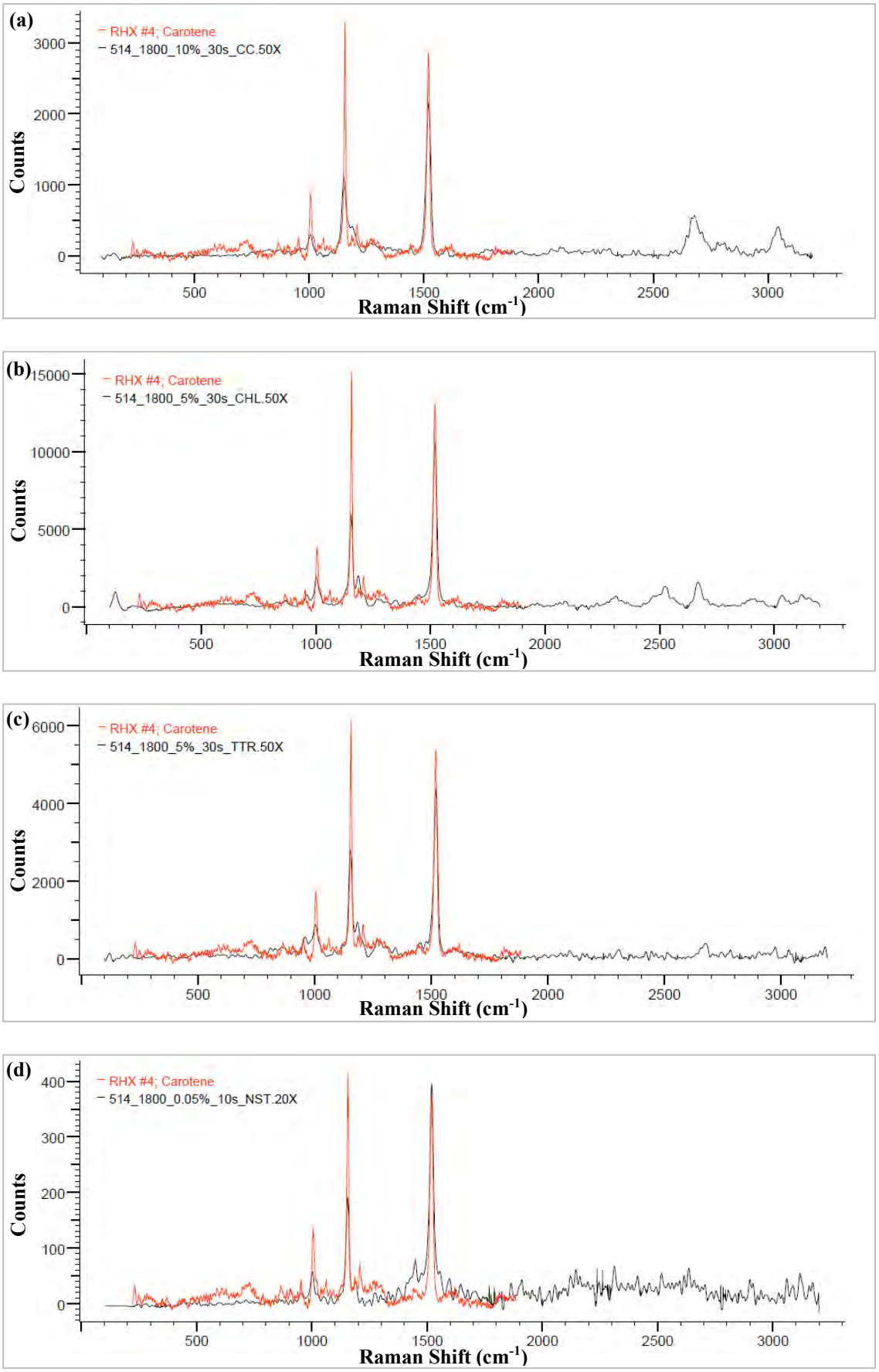

Figure 4.11: Raman spectra of carotene in (a) *C. calcitrans* (73% match); (b) *Chlorella* spp. (82% match); (c) *Tetraselmis* spp. (84% match); and (d) *Nostoc* spp. (72% match)

Moreover, the functional group analysis of the query spectrum was determined from the spectral analysis panel, and verified with the functional group database which was reported by Lin-Vien et al. (1991). The functional groups and the vibrational modes of the studied species are tabulated in Table 4.6.

Table 4.6: The functional group and the vibrational mode of the studied species, with its respective Raman shift.

Functional Group	Bond	Raman Shift (cm^{-1})	Intensity	Vibrational Mode	Studied species
Alcohol C(C)(C)C–OH	C–C–O	1100–1210	Medium-strong	Asymmetric stretching	All studied species
Hydrazide (PhCONHNHCOPh)	C–N–H	1525–1535	Weak	Deformation (Amide II)	All studied species
Phosphorus	P–O–C	970–1050	Medium-weak	Asymmetric stretching	All studied species
Alkane (Cyclopropyl)	C–H	1180–1200	Variable	Ring vibration (ring breathing)	*Chlorella* spp.
Ether (Epoxy)	CH_2	3030–3060	Medium-weak	Asymmetric stretching	*C. calcitrans*
Halosilane	SiF_3	945–980	Medium-weak	Asymmetric stretching	*Tetraselmis* spp.
Aromatics (Tetrasubstituted benzene)	Ring	1430–1465	Medium	Asymmetric stretching	*Nostoc* spp.

There are two types of vibrational mode in Raman scattering and IR absorption, namely stretching and bending. The stretching mode is either symmetric or asymmetric, while, bending or deformation mode is either in-plane or out-of-plane. In this study, the functional groups of the query spectrum consisted of a mixture of Raman and IR active vibrations, mostly IR active. The covalent bond of a molecule is IR active (Raman inactive) when vibrated in the asymmetric stretch or deformation, therefore, altering its dipole moment. In contrast, the covalent bond is Raman active (IR inactive) when vibrated in the symmetric stretch, therefore, affecting its polarizability.

The functional groups that fingerprinted the selected algae and cyanobacteria were determined. The functional groups obtained were the groups of alcohol, hydrazide, organophosphorus, cycloalkane, ether, halosilane and aromatics, as shown in Table 4.6. Alcohol, hydrazide and phosphorus group were characterised in all the studied species.

The C–C–O bond of tertiary alcohol was stretched asymmetrically. The tertiary alcohol is IR active (strong band) and Raman inactive (medium-strong band), corresponded at the wavenumber 1100–1210 cm^{-1}. Hydrazide has a similar chemical compound with amide. The mixture of deformation and stretching, produced a weak Raman band and a strong IR band of amide II (the stretch-bend vibration), corresponded at the wavenumber 1525–1535 cm^{-1}. The P–O–C bond of organophosphorus was stretched asymmetrically. The organophosphorus is IR active (strong band) and Raman inactive (medium-weak band), corresponded at the wavenumber 970–1050 cm^{-1}.

Furthermore, in *Chlorella* spp., the ring breathing of cyclopropyl is Raman active (IR inactive), corresponded at the wavenumber 1180–1200 cm^{-1}. An asymmetric stretching was observed in the CH_2 bond of cyclic 3-ring ether (epoxy or epoxide), corresponded at the wavenumber 3030–3060 cm^{-1}, and the SiF_3 bond of organohalosilane, corresponded at the wavenumber 945–980 cm^{-1}, which was characterised in *C. calcitrans* and *Tetraselmis* spp., respectively. Hence, both functional groups are IR active (Raman inactive). Lastly, in *Nostoc* spp., semicircle stretching was observed in the C–C bonds of a tetrasubstituted benzene ring, corresponded at the wavenumber 1430–1465 cm^{-1}. The semicircle stretch is asymmetric, hence, the spectrum is IR active (Raman inactive).

CHAPTER 5: DISCUSSION

5.1 Cell Density Measurement

The cell density measurements (Table 4.1) was calculated based on the manual cell counting by using a haemocytometer. The number of cells counted in the corner squares and the middle square grids may be miscalculated, as some cells were aggregated. This hinders the actual estimation of the cell count. Cell debris was absent in the culture flask and the cell viability was 100%. The nutrients from the growth media were adequate for the growth of the algae and cyanobacteria, and continuous subculture hinders the growth of unwanted microorganisms. As the conventional cell counting method is widely used in many labs, automated cell counters are the solution for accuracy in cell density.

5.2 Molecular Biomarkers

5.2.1 The p23SrV and 18Sr Biomarkers

5.2.1.1 DNA Extraction

The DNA of algae and cyanobacteria was extracted using the phenol-chloroform extraction method. Phenol-chloroform extraction was favoured over the commercial extraction kits, namely GF-1 plant DNA extraction kit and EasyPure bacteria genomic DNA kit, due to the high concentration and the high yield production of nucleic acids. In commercial extraction kits, the A260/A280 ratio was lower than 1.80 and a very low yield of nucleic acids (less than 10 ng/µl) were produced. This signifies the presence of contamination in the extracted nucleic acids, especially in cyanobacteria.

As cyanobacteria have thick peptidoglycan layer compared to other gram-negative bacteria, the lysis buffer of the commercial extraction kits was less efficient in lysing the peptidoglycan layer (Morin et al., 2010; Hoiczyk & Hansel, 2000). With SDS incorporated in the phenol-chloroform extraction, the cell wall of cyanobacteria was digested, and high molecular weight of DNA was extracted with good purity (Morin et al., 2010; Ausubel et al., 2003; Hoiczyk & Hansel, 2000).

Based on Table 4.2, the extracted DNA resulted in good purity. The A260/A280 ratio lower than 1.80, signified the presence of protein or phenol contamination, absorbed at 280 nm wavelength (Desjardins & Conklin, 2010). The A260/A230 ratio is the secondary measurement of nucleic acids, and any values lower than 2.0, signified contamination, absorbed at 230 nm wavelength (Desjardins & Conklin, 2010).

5.2.1.2 DNA Amplification

The p23SrV and 18Sr biomarkers successfully amplified the DNA of the selected algae and cyanobacteria. The bands observed were intact and no primer-dimer was produced. This signifies that the designed primer pair was specific and complementary to the DNA template, and the primer pair annealed at the right temperature (Nonis et al., 2011; Brownie et al., 1997). Gradient PCR determines the optimal annealing temperature, and no bands were observed, when the temperature is higher or lower than the annealing temperature range, that was stated in Table 3.2. Likewise, there was no contamination in the master mix, as the bands were absent in the negative control.

5.2.1.3 Phylogenetic Tree and Median-Joining Network Analysis

The diversity of the plastid genes was studied in the selected algae and cyanobacteria via the p23SrV biomarker. The p23SrV gene fragment serves as a universal biomarker in determining the taxonomic lineage of algae groups and cyanobacteria (Sherwood & Presting, 2007; Presting, 2006). This was validated from the Neighbor-Joining tree in Figure 4.4, as the studied species were grouped in its expected clades or lineages. *G. violaceus*, a sister group of cyanobacteria, was selected as the outgroup species. It is a model organism that has diverged from cyanobacteria, before the evolution of thylakoid membranes and plastids, yet, capable of performing photosynthesis in absence of the photosynthetic organelles (Saw et al., 2013; Mareš et al., 2013; Mimuro et al., 2010).

Based on the Neighbor-Joining tree in Figure 4.4, *Tetraselmis* spp. was closely related to *T. chuii* with bootstrap support of 79%. The genetic distances between both strains were 0.004, hence, *Tetraselmis* spp. was characterised as *T. chuii*. Whereas, *Nostoc* spp. was conspecific to *N. commune* with bootstrap support of 100%. The genetic distances between both strains were null, hence, *Nostoc* spp. was characterised as *N. commune*. Similarly, *Chlorella* spp. was conspecific to *Parachlorella* spp. with bootstrap support of 99%. The genetic distances between both strains were null, hence, *Chlorella* spp. was characterised as *Parachlorella* spp.

Krienitz et al. (2004) have reported that the *Chlorella* clade and the *Parachlorella* clade are the two sister groups of Family Chlorellaceae. The sister clade of *Parachlorella* spp. was comprised of *Chlorella vulgaris* and *Chlorella variabilis* with bootstrap support of 100%. The codon GTT encodes for Valine, while, the codon GCT encodes for Alanine. The substitution of Thymine (T) to Cytosine (C), at site 47, caused the alteration of amino acids from Valine to Alanine, therefore, the change of *C. vulgaris* to *C. variabilis*.

Alternatively, the Neighbor-Joining tree in Figure 4.6 shows a better separation of the Chromista lineage. Both *Chlorella* spp. and *Tetraselmis* spp. from the Phylum Chlorophyta were grouped, meanwhile, the diatom *C. calcitrans* was separated into a new clade from *I. galbana*. *C. calcitrans* is a diatom classified under Phylum Bacillariophyta, while, *I. galbana* is a coccolithophore classified under Phylum Haptophyta (Guiry et al., 2014). However, the 18Sr biomarker is only an additional biomarker that characterised the taxonomic lineage of algae, since, the p23SrV biomarker is more versatile in characterising the taxonomic lineage of both prokaryotic and eukaryotic organisms.

Moreover, from the median-joining network analysis, four distinct haplogroups and two distinct haplogroups were observed in Figures 4.5 and 4.7, respectively. The haplotype in each population was highly endemic and distinct. The median vector represented the ancestry point before a species descends from its common ancestry (Forster, 2015). The mutation rate was higher for the descendant of brown algae from its median vector, compared to the green algae and cyanobacteria (Figures 4.5 and 4.7). This is due to the multiple endosymbioses that increased the complexity of the cell structure and organelles of brown algae, upon evolution (Cavalier-Smith, 2018; Gould et al., 2008; McFadden, 2001). However, a mismatch distribution analysis was not conducted in this study as the number of species grouped in each haplotype was limited.

5.2.2 mcy Gene Cluster

The mcy gene cluster was not amplified in the cyanobacteria, *M. aeruginosa* and *Nostoc* spp., as shown by the absence of bands at the expected amplicon size. Since the biosynthesis of microcystin is synthesised via a series of enzymatic reactions, each domain must be activated for the expression of microcystin to take place, starting from the precursor mcyG, followed by mcyD, mcyE, mcyA, mcyB, and finally, mcyC (Neilan et al., 2008; Dittmann & Borner, 2005; Tillett et al., 2000). In this study, these mcy gene clusters may have lost or not expressed, therefore, microcystin was not produced. If this gene cluster is completely lost, cyanobacteria might lose its ability to biosynthesise microcystin (Kurmayer & Christiansen, 2009). CCAP has also reported that both of the cyanobacteria strains were souced as non-toxic strains.

Kurmayer & Christiansen (2009) have reported that the loss of the mcy gene cluster is due to gene transfer or insertion and deletion events. Transposases that were found at the 3' end undergo horizontal gene transfer with the mcy gene cluster. Another hypothesis is the insertion and deletion events which caused a patchy distribution of the mcy gene cluster and gene loss, eventually. The gene loss might have occurred at a later evolutionary timescale, as the mcy gene cluster is always existent in all the cyanobacteria ancestry (Kurmayer & Christiansen, 2009).

5.3 GC-MS

The GC column allows the separation of compounds based on its volatility and polarity, whereby, the organic compounds with higher volatility resulted in shorter retention time (Adesalu et al., 2016). Nevertheless, 3,5-octadiyne, 2,7-bis[t-butoxycarbonyl)amino]-1,8-diphenyl-, was eluted first in *M. aeruginosa*, although with the lowest volatility. This compound is highly polar, with the largest topological polar surface area, at 76.7 $Å^2$, as reported in PubChem (Kim et al., 2018a; Caron & Ermondi, 2016). Another factor is the non-polar DB-5 capillary column, which has a stronger affinity with the non-polar compounds. Therefore, the non-polar compounds have a longer retention time than polar compounds.

Based on the GC-MS chromatogram in Figures 4.8 and 4.9, a limited number of organic compounds were characterised. The studies reported by Adesalu et al. (2016); Devi & Mehta (2016); Sharmila et al. (2016); and Řezanka et al. (2003), incorporated fatty acid methyl esters extraction, which characterised various organic compounds, namely the derivatives of alcohol, fatty acid, hydrocarbon and siloxane. However, this solvent extraction required lengthy sample preparation and expensive chemicals. Hence, in this study, only hexane was used as the organic solvent, which reduced the sample preparation time, yet, eluting similar organic compounds to the reported literature.

The organic compounds characterised in the selected algae and cyanobacteria are utilised in biofuels production, cosmetics, industrial lubricants and paint coatings, as well as, some compounds are toxic. The hazard classification was reported by the European Chemicals Agency (ECHA).

Cyclohexasiloxane, dodecamethyl- (PubChem Identifier: CID 10911) is an odourless clear oil that is used in personal care and household products. It is synthesised as an emollient in cosmetics, moisturisers, hair spray, breast implants, household sanitation, paint and varnishes (Horii & Kannan, 2008). This compound is manufactured as industrial lubricants and adhesives (Kaj et al., 2005). Cyclohexasiloxane, dodecamethyl- is an essential component of biofuels, which was also characterised by Sharmila et al. (2016).

1-hexanol, 2-ethyl- (PubChem Identifier: CID 7720) is a colourless liquid with an aromatic odour. It is used as a flavouring agent, lubricants, paint coatings, and as a solvent in manufacturing soft polyvinylchloride (PVC), resins and dyes of fabrics (Bahrmann et al., 2013). Nevertheless, this compound is moderately toxic with a lethal dose (LD_{50}) of 0.5-5 gm/kg in human and classified as an irritant (Kim et al., 2018a). The skin, eye and the respiratory tract was irritated, nausea and dizziness upon inhalation, and lead to celiac disease or ulcerative colitis (Francavilla et al., 2014).

Furthermore, phenol, 2,4-bis(1,1-dimethylethyl)- (PubChem Identifier: CID 7311), a whitish-yellow powder, is commonly used as an antioxidant in aviation fuels, and a UV stabiliser in PVC and polyolefins (Fiege et al., 2000). However, this compound is corrosive, irritant and an environmental hazard, with LD_{50} of 25 mg/kg in mouse. Upon in contact, one suffers from skin corrosion and damaged eye, irritated respiratory tract, and prolonged toxicity effect in aquatic species (Kim et al., 2018a). Similarly, phenol, 2,5-bis(1,1-dimethylethyl)- (PubChem Identifier: CID 79983) inhibit the calcium signalling in rabbit, and irritated the skin and the respiratory tract (Kim et al., 2018a).

2-propen-1-one, 3-(4-nitrophenyl)-1-phenyl- (PubChem Identifier: CID 14654) is used as drugs or anti-inflammatory agents for the treatment of human immunodeficiency viruses and neurodegenerative disorders (Kim et al., 2018a). Besides, nonadecane (PubChem Identifier: CID 12401) is a white waxy solid that is synthesised as paraffin waxes, candles, biopesticides and detergent (Adesalu et al., 2016; Schmidt et al., 2014). Nonadecane is also used as aviation fuels, lubricating oil in engines and turbines, and as an anti-corrosive agent (Adesalu et al., 2016). The detection of nonadecane from algae and cyanobacteria were also reported by Adesalu et al. (2016) and Devi & Mehta (2016).

The effect of 3,5-Octadiyne, 2,7-bis[t-butoxycarbonyl)amino]-1,8-diphenyl- (PubChem Identifier: CID 546741) and 2-(Acetoxymethyl)-3-(methoxycarbonyl) biphenylene (PubChem Identifier: CID 610255) are still unknown, as there is no available database in PubChem and ECHA, regarding on its uses and toxicity. In short, all these organic compounds have their uses and dangers. If introduced in excessive or in high concentration into the environment, unintentionally or vice versa, it will just bring in more harm than good to humans, ultimately.

5.4 Raman Spectroscopy

The Raman signatures of carotenoids are found mainly at three peaks, corresponded at wavenumber 1010 cm^{-1}, 1155 cm^{-1} and 1520 cm^{-1} (Baqué et al., 2018; Parab & Tomar, 2012; Pilát et al., 2012). The Raman spectra of *C. calcitrans*, *Chlorella* spp., *Tetraselmis* spp., and *Nostoc* spp. strongly corresponded at these mentioned peaks, with the strongest peak at around 1520 cm^{-1}. In addition, the Raman signatures of saffron also produced peaks like carotenoids. Saffron is a Mediterranean spice that has many beneficial usages in ayurvedic medicines, cancer treatment, antidepressant drugs and food colourings (Anuar et al., 2018). The bio-compounds of saffron, namely crocetin, crocin and safranal, are characterised as the derivatives of carotenoids (Anuar et al., 2018; Lou et al., 2016).

The functional groups, namely alcohol, hydrazide, organophosphorus, cycloalkane, ether, halosilane and aromatics, were characterised (Table 4.6). The tertiary alcohol is IR active (Raman inactive) due to the higher electronegativity of the C–O bond than the C–C bond, hence, the dipole moment is altered during the asymmetric stretch (Lin-Vien et al., 1991). The in-plane deformation of the C–N–H bond and the stretching of the C–N bond, produced amide II (the stretch-bend vibration) in trans-cyclic amide (hydrazide) (Lin-Vien et al., 1991). In organophosphorus, the O–C bond is stretched more than the P–O bond, hence, the dipole moment is altered (Lin-Vien et al., 1991).

The ring vibration of cyclopropyl is Raman active (IR inactive), as the ring breathing is symmetric and polarised strongly (Lin-Vien et al., 1991). The Raman shift frequency will decrease in larger cycloalkanes, as the ring strain is reduced and the stability is increased, in larger cycloalkane (Lin-Vien et al., 1991). Moreover, halosilane produces siloxane when in contact with water (Lin-Vien et al., 1991), and cyclohexasiloxane (the derivative of siloxane) was eluted in GC-MS from *Tetraselmis* spp. Lastly, in *Nostoc* spp.,

the equally distributed C–C bonds in the benzene ring vibrated in two modes, the quadrant stretch or the semicircle stretch (Lin-Vien et al., 1991). At the wavenumber 1430–1465 cm^{-1}, semicircle stretch was observed, whereby, the C–C bonds in one semicircle region is stretched, while, the other is contracted (Lin-Vien et al., 1991).

The noise signal of the Raman spectrum of *Nostoc* spp. (Appendix I), was high, at the higher wavenumber (1600–3000 cm^{-1}). This interfered with the characterisation of the functional groups at these frequencies. The noise produced is due to the fluorescence of the elastic scattered light, which is stronger than the Raman scattering, or the dark current that is produced at an increased temperature of the detector (Smulko et al., 2015). The fluorescence noise can be reduced through the increase of exposure time of the visible light laser (514 nm) (Smulko et al., 2015). The magnification of the objective lens and the slit aperture can also be increased for a lower depth-of-focus of the region of interest (Lázaro et al., 2009). Despite the noise, at the lower wavenumber (the fingerprinting region), the peak is manageable for analysis.

The Raman analysis in this study provides an insight into the pigment analysis of algae and cyanobacteria, with its respective vibrational properties. It is possible to extract crocetin, which is the main pigment of saffron, from algae and cyanobacteria, instead of from the expensive and limited natural saffron. This had been proven in the transgenic *C. vulgaris* for the production of crocetin (Anuar et al., 2018; Lou et al., 2016).

CHAPTER 6: CONCLUSION AND RECOMMENDATIONS

6.1 Conclusion

In summary, this study represented the selected bioanalytical approaches that simplified the characterisation of the selected algae and cyanobacteria. As such is the universal p23SrV biomarker that differentiated the taxonomic clades of algae (brown and green algae) and cyanobacteria. This biomarker eliminated the use of the 16S rRNA, 18S rRNA or the ITS gene region primers that were established in past years. *Chlorella* spp. was conspecific to *Parachlorella* spp., *Tetraselmis* spp. was closely related to *T. chuii*, and *Nostoc* spp. was conspecific to *N. commune* The mcy gene cluster was not expressed in both of the cyanobacteria species, thus, may have lost its ability to produce microcystin.

The characterisation of organic compounds via GC-MS can be incorporated in industrial applications such as biofuels, cosmetics and skincare, fabrications of polymers and plastics, flavouring agents, lubricants, paint coatings, and paraffin waxes. Lastly, the functional group vibrations and the pigment analysis obtained from the Raman scattering provided fingerprinting characteristics, which corresponded to saffron and carotene. Raman spectroscopy is non-destructive and offers a direct measurement of analysis, with hassle-free of sample preparation. Therefore, perfect to be miniaturised into a handheld device for field applications in future.

6.2 Recommendations

Pure cultures of the selected algae and cyanobacteria were sourced from the culture collection centre. Environmental samples were not studied, as isolation and morphological identification is a hassle, which might be analysed as false-positives. Some algae cultures died off in the long run of continued propagation, which hinders further characterisation analysis. Proper facilities for the cultivation of algae is recommended. As for future studies, the p23SrV biomarker can be tested in the aquaculture lake that is positive of algae bloom for environmental monitoring. Further studies on the expression of the mcy gene cluster using a qPCR will give a new insight. The isolation of the organic compounds from the algae and cyanobacteria extract for industrial commercialisations is highly suggested. Last but not least, further characterisation studies in Raman spectroscopy using field samples is recommended.

REFERENCES

Abd Rahman, A. R., Che Cob, Z., Jamari, Z., Mohamed, A. M., Toda, T., & Haji Ross, O. (2018). The effects of microalgae as live food for *Brachionus plicatilis* (rotifer) in intensive culture system. *Tropical Life Sciences Research*, *29*(1), 127–138.

Abdel-Raouf, N., Al-Homaidan, A. A., & Ibraheem, I. B. M. (2012). Agricultural importance of algae. *African Journal of Biotechnology*, *11*(54), 11648–11658.

Abdu Rahman, N., Khatoon, H., Yusuf, N., Banerjee, S., Haris, N. A., Lananan, F., & Tomoyo, K. (2017). *Tetraselmis chuii* biomass as a potential feed additive to improve survival and oxidative stress status of Pacific white-leg shrimp *Litopenaeus vannamei* postlarva. *International Aquatic Research*, *9*(3), 235–247.

Adams, D. G., & Duggan, P. S. (1999). Tansley Review No. 107: Heterocyst and akinete differentiation in cyanobacteria. *The New Phytologist*, *144*(1), 3–33.

Adams, V. D., Renk, R. R., Cowan, P. A., & Porcella, D. B. (1975). *Naturally occurring organic compounds and algal growth in a eutrophic lake*. Retrieved on August 11, 2019 from https://digitalcommons.usu.edu/water_rep/653/

Adesalu, T. A., Temenu, T. O., & Julius, M. L. (2016). Molecular characterization, lipid analysis and GC-MS determination of bioactive compounds identified in a West African strain of the green alga *Oedogonium* (Chlorophyta). *Journal of Pharmacognosy and Phytochemistry*, *5*(6), 1–6.

Ahmed, A., Rushworth, J. V., Hirst, N. A., & Millner, P. A. (2014). Biosensors for whole-cell bacterial detection. *Clinical Microbiology Reviews*, *27*(3), 631–646.

Alunni-Fabbroni, M., & Sandri, M. T. (2010). Circulating tumour cells in clinical practice: Methods of detection and possible characterization. *Methods*, *50*(4), 289–297.

Anuar, N., Mat Taha, R., Mahmad, N., & Othman, R. (2018). Identification of crocin, crocetin and zeaxanthin in *Crocus sativus* grown under controlled environment in Malaysia. *Pigment & Resin Technology*, *47*(6), 502–506.

Arruda, S. R., Pereira, D. G., Silva-Castro, M. M., Brito, M. G., & Waldschmidt, A. M. (2017). An optimized protocol for DNA extraction in plants with a high content of secondary metabolites, based on leaves of *Mimosa tenuiflora* (Willd.) Poir. (Leguminosae). *Genetics and Molecular Research*, *16*(3), 1–9.

Ausubel, F. M., Brent, R., Kingston, R. E., Moore, D. D., Seidman, J. G., Smith, J. A., & Struhl K. (Eds.). (2003). *Current protocols in molecular biology*. New Jersey, US: John Wiley & Sons.

Bahrmann, H., Hahn, H. D., Mayer, D., & Frey, G. D. (2013). 2-Ethylhexanol. In *Ullmann's encyclopedia of industrial chemistry* (pp. 1–6). Weinheim, Germany: Wiley-VCH Verlag.

Banack, S. A., & Cox, P. A. (2003). Distribution of the neurotoxic nonprotein amino acid BMAA in *Cycas micronesica*. *Botanical Journal of the Linnean Society*, *143*(2), 165–168.

Baqué, M., Hanke, F., Böttger, U., Leya, T., Moeller, R., & de Vera, J. P. (2018). Protection of cyanobacterial carotenoids' Raman signatures by Martian mineral analogues after high-dose gamma irradiation. *Journal of Raman Spectroscopy*, *49*(10), 1617–1627.

Blank, C. E., & Sanchez-Baracaldo, P. (2010). Timing of morphological and ecological innovations in the cyanobacteria: A key to understanding the rise in atmospheric oxygen. *Geobiology*, *8*(1), 1–23.

Brookes, J. D., & Ganf, G. G. (2001). Variations in the buoyancy response of *Microcystis aeruginosa* to nitrogen, phosphorus and light. *Journal of Plankton Research*, *23*(12), 1399–1411.

Brownie, J., Shawcross, S., Theaker, J., Whitcombe, D., Ferrie, R., Newton, C., & Little, S. (1997). The elimination of primer-dimer accumulation in PCR. *Nucleic Acids Research*, *25*(16), 3235–3241.

Buchanan, R. E., & Gibbons, N. E. (1974). *Bergey's manual of determinative bacteriology* (8th ed.). Baltimore, US: Williams and Wilkins Co.

Carmichael, W. W., Azevedo, S. M. F. O., An, J. S., Molica, R. J. R., Jochimsen, E. M., Lau, S., … Eaglesham, G. K. (2001). Human fatalities from cyanobacteria: Chemical and biological evidence for cyanotoxins. *Environmental Health Perspectives*, *109*(7), 663–668.

Carpenter, A. E., Jones, T. R., Lamprecht, M. R., Clarke, C., Kang, I. H., Friman, O., … Sabatini, D. M. (2006). Cellprofiler: Image analysis software for identifying and quantifying cell phenotypes. *Genome Biology*, *7*(10), 1–11.

Caron, G., & Ermondi, G. (2016). Molecular descriptors for polarity: The need of going beyond polar surface area. *Future Medicinal Chemistry*, *8*(17), 1–4.

Cavalier-Smith, T. (2018). Kingdom Chromista and its eight phyla: A new synthesis emphasising periplastid protein targeting, cytoskeletal and periplastid evolution, and ancient divergences. *Protoplasma*, *255*(1), 297–357.

Connell, L. (2002). Rapid identification of marine algae (Raphidophyceae) using three-primer PCR amplification of nuclear internal transcribed spacer (ITS) regions from fresh and archived material. *Phycologia*, *41*(1), 15–21.

Cras, J. J., Rowe-Taitt, C. A., Nivens, D. A., & Ligler, F. S. (1999). Comparison of chemical cleaning methods of glass in preparation for silanization. *Biosensors and Bioelectronics*, *14*(8–9), 683–688.

Demirbas, A., & Demirbas, M. F. (2011). Importance of algae oil as a source of biodiesel. *Energy Conversion and Management*, *52*(1), 163–170.

Desjardins, P., & Conklin, D. (2010). Nanodrop microvolume quantitation of nucleic acids. *Journal of Visualized Experiments*, *45*, 1–5.

Deusch, O., Landan, G., Roettger, M., Gruenheit, N., Kowallik, K. V., Allen, J. F., ... Dagan, T. (2008). Genes of cyanobacterial origin in plant nuclear genomes point to a heterocyst-forming plastid ancestor. *Molecular Biology and Evolution*, *25*(4), 748–761.

Devi, K. M., & Mehta, S. K. (2016). Antimicrobial activity and GC-MS analysis of freshwater cyanobacterium, *Fisherella ambigua*. *World Journal of Pharmaceutical and Medical Research*, 2(5), 199–208.

Dittmann, E., & Börner, T. (2005). Genetic contributions to the risk assessment of microcystin in the environment. *Toxicology and Applied Pharmacology*, *203*(3), 192–200.

Duong, V. T., Ahmed, F., Thomas-Hall, S. R., Quigley, S., Nowak, E., & Schenk, P. M. (2015). High protein- and high lipid-producing microalgae from northern Australia as potential feedstock for animal feed and biodiesel. *Frontiers in Bioengineering and Biotechnology*, *3*(53), 1–7.

Eman, A. M., Laila, A. F., Zeinab, K. A. A., Nesreen, A. F., Samy, B. E., & Rawheya, A. S. E. D. (2016). Cultivation of microalgae using municipal wastewater as a nutritional source. *Journal of Algal Biomass Utilization*, *7*(1), 78–85.

Ettoumi, A., El Khalloufi, F., El Ghazali, I., Oudra, B., Amrani, A., Nasri, H., & Bouaïcha, N. (2011). Bioaccumulation of cyanobacterial toxins in aquatic organisms and its consequences for public health. In G. Kattel (Ed.), *Zooplankton and phytoplankton: Types, characteristics and ecology* (pp. 1–33). New York, US: Nova Science Publishers.

Falconer, I. R., & Humpage, A. R. (2006). Cyanobacterial (blue-green algal) toxins in water supplies: Cylindrospermopsins. *Environmental Toxicology*, *21*(4), 299–304.

Ferrão-Filho, A. D. S., & Kozlowsky-Suzuki, B. (2011). Cyanotoxins: Bioaccumulation and effects on aquatic animals. *Marine Drugs*, *9*(12), 2729–2772.

Fiege, H., Voges, H. W., Hamamoto, T., Umemura, S., Iwata, T., Miki, H., … Paulus, W. (2000). Phenol derivatives. In *Ullmann's encyclopedia of industrial chemistry* (pp. 521–582). Weinheim, Germany: Wiley-VCH Verlag.

Fiore, M. F., Moon, D. H., Tsai, S. M., Lee, H., & Trevors, J. T. (2000). Miniprep DNA isolation from unicellular and filamentous cyanobacteria. *Journal of Microbiological Methods*, *39*(2), 159–169.

Fischer, W. J., Hitzfeld, B. C., Tencalla, F., Eriksson, J. E., Mikhailov, A., & Dietrich, D. R. (2000). Microcystin-LR toxicodynamics, induced pathology, and immunohistochemical localization in livers of blue-green algae exposed rainbow trout (*Oncorhynchus mykiss*). *Toxicological Sciences*, *54*(2), 365–373.

Forster, M. (2015). *Network 5.0.0.0 user guide*. Retrieved on August 11, 2019 from http://www.fluxus-engineering.com/Network5000_user_guide.pdf

Fournier, P. E., Drancourt, M., Colson, P., Rolain, J. M., Scola, B. L., & Raoult, D. (2013). Modern clinical microbiology: New challenges and solutions. *Nature Reviews Microbiology*, *11*(8), 574–585.

Francavilla, R., Ercolini, D., Piccolo, M., Vannini, L., Siragusa, S., Filippis, F. D., ... Gobbetti, M. (2014). Salivary microbiota and metabolome associated with celiac disease. *Applied and Environmental Microbiology*, *80*(11), 3416–3425.

Friedl, T. & O'Kelly, C. J. (2002). Phylogenetic relationships of green algae assigned to the genus *Planophila* (Chlorophyta): Evidence from 18S rDNA sequence data and ultrastructure. *European Journal of Phycology*, *37*(3), 373–384.

Furuhashi, T., & Weckwerth, W. (2013). Introduction to lipid (FAME) analysis in algae using gas chromatography-mass spectrometry. In W. Weckwerth & G. Kahl (Eds.), *The handbook of plant metabolomics* (pp. 215–225). Weinheim, Germany: Wiley-VCH Verlag.

Gould, S. B., Waller, R. F., & McFadden, G. I. (2008). Plastid evolution. *Annual Review of Plant Biology*, *59*, 491–517.

Guiry, M. D., Guiry, G. M., Morrison, L., Rindi, F., Miranda, S. V., Mathieson, A. C., ... Garbary, D. J. (2014). Algaebase: An on-line resource for algae. *Cryptogamie Algologie*, *35*(2), 105–115.

Hoiczyk, E., & Hansel, A. (2000). Cyanobacterial cell walls: News from an unusual prokaryotic envelope. *Journal of Bacteriology*, *182*(5), 1191–1199.

Horii, Y., & Kannan, K. (2008). Survey of organosilicone compounds, including cyclic and linear siloxanes, in personal-care and household products. *Archives of Environmental Contamination and Toxicology*, *55*(4), 701–710.

Hosseini, S., Vázquez-Villegas, P., Rito-Palomares, M., & Martinez-Chapa, S. O. (2018). Advantages, disadvantages and modifications of conventional ELISA. In *Enzyme-linked immunosorbent assay (ELISA) from A to Z (*pp. 67–115). Springer, Singapore.

Ishida, T., Watanabe, M. M., Sugiyama, J., & Yokota, A. (2001). Evidence for polyphyletic origin of the members of the orders of Oscillatoriales and Pleurocapsales as determined by 16S rDNA analysis. *FEMS Microbiology Letters*, *201*(1), 79–82.

Jehlička, J., Edwards, H. G., & Oren, A. (2014). Raman spectroscopy of microbial pigments. *Applied and Environmental Microbiology*, *80*(11), 3286–3295.

Kaj, L., Schlabach, M., Andersson, J., Cousins, A. P., Schmidbauer, N., & Brorström-Lundén, E. (2005). *Siloxanes in the Nordic environment*. Copenhagen, Denmark: Nordic Council of Ministers.

Kaur, H., Bhagwat, S. R., Sharma, T. K., & Kumar, A. (2018). Analytical techniques for characterization of biological molecules – proteins and aptamers/oligonucleotides. *Bioanalysis*, *11*(2), 1–15.

Khatoon, H., Abdu Rahman, N., Banerjee, S., Harun, N., Suleiman, S. S., Zakaria, N. H., ... Endut, A. (2014). Effects of different salinities and pH on the growth and proximate composition of *Nannochloropsis* sp. and *Tetraselmis* sp. isolated from South China Sea cultured under control and natural condition. *International Biodeterioration & Biodegradation*, *95*, 11–18.

Kim, S., Chen, J., Cheng, T., Gindulyte, A., He, J., He, S., ... Bolton, E. E. (2018a). Pubchem 2019 update: Improved access to chemical data. *Nucleic Acids Research*, *47*(D1), D1102–D1109.

Kim, S. M., Kang, S. W., Kwon, O. N., Chung, D., & Pan, C. H. (2012b). Fucoxanthin as a major carotenoid in *Isochrysis* aff. *galbana*: Characterization of extraction for commercial application. *Journal of the Korean Society for Applied Biological Chemistry*, *55*(4), 477–483.

Krienitz, L., Hegewald, E. H., Hepperle, D., Huss, V. A. R., Rohr, T., & Wolf, M. (2004). Phylogenetic relationship of *Chlorella* and *Parachlorella* gen. nov. (Chlorophyta, Trebouxiophyceae). *Phycologia*, *43*(5), 529–542.

Kumar, K., Mella-Herrera, R. A., & Golden, J. W. (2010). Cyanobacterial heterocysts. *Cold Spring Harbor Perspectives in Biology*, *2*(4), 1–19.

Kurmayer, R., & Christiansen, G. (2009). The genetic basis of toxin production in cyanobacteria. *Freshwater Reviews*, *2*(1), 31–50.

Lázaro, J. C., Pacheco, M. T. T., Rodrigues, K. C., José de Lima, C., Moreira, L. M., Villaverde, A. B., & Silveira Jr, L. (2009). Optimizing the Raman signal for characterizing organic samples: The effect of slit aperture and exposure time. *Journal of Spectroscopy*, *23*(2), 71–80.

Lazcka, O., Javier Del Campo, F., & Xavier Muñoz, F.. (2007). Pathogen detection: A perspective of traditional methods and biosensors. *Biosensors and Bioelectronics*, *22*(7), 1205–1217.

Lembi, C. A., & Waaland, J. R. (1988). *Algae and human affairs*. New York, US: Cambridge University Press.

Lim, P. T., Usup, G., & Leaw, C. P. (2012). Harmful algal blooms in Malaysian waters. *Sains Malaysiana*, *41*(12), 1509–1515.

Lin-Vien, D., Colthup, N. B., Fateley, W. G., & Grasselli, J. G. (1991). *The handbook of infrared and Raman characteristic frequencies of organic molecules*. Amsterdam, Netherlands: Elsevier.

Loftin, K., Graham, J., Rosen, B., & St. Amand, A. (2010). Analytical methods for cyanotoxin detection and impacts on data interpretation. In *Guidelines for design, sampling, analysis and interpretation for cyanobacterial toxin studies*. Paper presented at the National Water Quality Monitoring Conference, Denver, Colorado, USA.

Lou, S., Wang, L., He, L., Wang, Z., Wang, G., & Lin, X. (2016). Production of crocetin in transgenic *Chlorella vulgaris* expressing genes *crtRB* and *ZCD1*. *Journal of Applied Phycology*, *28*(3), 1657–1665.

Louis, K. S., & Siegel, A. C. (2011). Cell viability analysis using trypan blue: Manual and automated methods. In M.J. Stoddart (Ed.), *Mammalian cell viability: Methods and protocols* (pp. 7–12). New York, US: Humana Press.

Ma, J., Wang, P. W., Yao, D., Wang, Y. P., Yan, W., & Guan, S. C. (2011). Single-primer PCR correction: A strategy for false-positive exclusion. *Genetics and Molecular Research*, *10*(1), 150–159.

Maneveldt, G. W., & Keats, D. W. (2004). Chromista. In *Encyclopedia of life sciences* (pp. 1–16). New Jersey, US: John Wiley & Sons.

Mareš, J., Hrouzek, P., Kaňa, R., Ventura, S., Strunecký, O., & Komárek, J. (2013). The primitive thylakoid-less cyanobacterium *Gloeobacter* is a common rock-dwelling organism. *PLOS ONE*, *8*(6), 1–11.

McFadden, G. I. (2001). Primary and secondary endosymbiosis and the origin of plastids. *Journal of Phycology*, *37*(6), 951–959.

Mikalsen, B., Boison, G., Skulberg, O. M., Fastner, J., Davies, W., Gabrielsen, T. M., … Jakobsen, K. S. (2003). Natural variation in the microcystin synthetase operon *mcyABC* and impact on microcystin production in *microcystis* strains. *Journal of Bacteriology*, *185*(9), 2774–2785.

Mimuro, M., Yokono, M., & Akimoto, S. (2010). Variations in photosystem I properties in the primordial cyanobacterium *Gloeobacter violaceus* PCC 7421. *Photochemistry and Photobiology*, *86*(1), 62–69.

Mohebbi, F., Hafezieh, M., Seidgar, M., Hosseinzadeh Sahhafi, H., Mohsenpour Azari, A., & Ahmadi, R. (2016). The growth, survival rate and reproductive characteristics of *Artemia urmiana* fed by *Dunaliella tertiolecta*, *Tetraselmis suecica*, *Nannochloropsis oculata*, *Chaetoceros* sp., *Chlorella* sp. and *Spirolina* sp. as feeding microalgae. *Iranian Journal of Fisheries Sciences*, *15*(2), 727–737.

Monson, C. S., Banack, S. A., & Cox, P. A. (2003). Conservation implications of Chamorro consumption of flying foxes as a possible cause of amyotrophic lateral sclerosis–Parkinsonism dementia complex in Guam. *Conservation Biology*, *17*(3), 678–686.

Morin, N., Vallaeys, T., Hendrickx, L., Natalie, L., & Wilmotte, A. (2010). An efficient DNA isolation protocol for filamentous cyanobacteria of the genus *Arthrospira*. *Journal of Microbiological Methods*, *80*(2), 148–154.

Murch, S. J., Cox, P. A., & Banack, S. A. (2004). A mechanism for slow release of biomagnified cyanobacterial neurotoxins and neurodegenerative disease in Guam. *Proceedings of the National Academy of Sciences of the United States of America*, *101*(33), 12228–12231.

Neilan, B. A., Pearson, L. A., Moffitt, M. C., Mihali, K. T., Kaebernick, M., Kellmann, R., & Pomati, F. (2008). The genetics and genomics of cyanobacterial toxicity. In H.K. Hudnell (Ed.), *Cyanobacterial harmful algal blooms: State of the science and research needs* (pp. 417–452). New York, US: Springer Science & Business Media.

Nonis, A., Scortegagna, M., Nonis, A., & Ruperti, B. (2011). PRaTo: A web-tool to select optimal primer pairs for qPCR. *Biochemical and Biophysical Research Communications*, *415*(4), 707–708.

Norris, R. E., Hori, T., & Chihara, M. (1980). Revision of the genus *Tetraselmis* (class Prasinophyceae). *The Botanical Magazine Tokyo*, *93*(4), 317–339.

Nozaki, H., Matsuzaki, M., Misumi, O., Kuroiwa, H., Hasegawa, M., Higashiyama, T., ... Kuroiwa, T. (2004). Cyanobacterial genes transmitted to the nucleus before divergence of red algae in the Chromista. *Journal of Molecular Evolution*, *59*(1), 103–113.

Ouahid, Y., Pérez-Silva, G., & Campo, F. F. D. (2005). Identification of potentially toxic environmental *Microcystis* by individual and multiple PCR amplification of specific microcystin synthetase gene regions. *Environmental Toxicology*, *20*(3), 235–242.

Pakala, R., & Waksman, R. (2011). Currently available methods for platelet function analysis: Advantages and disadvantages. *Cardiovascular Revascularization Medicine*, *12*(5), 312–322.

Parab, N. D. T., & Tomar, V. (2012). Raman spectroscopy of algae: A review. *Journal of Nanomedicine & Nanotechnology*, *3*(2), 1–7.

Pavlopoulos, G. A., Soldatos, T. G., Barbosa-Silva, A., & Schneider, R. (2010). A reference guide for tree analysis and visualization. *BioData Mining*, *3*(1), 1–16.

Pilát, Z., Bernatová, S., Ježek, J., Šerý, M., Samek, O., Zemánek, P., ... Trtílek, M. (2012). Raman microspectroscopy of algal lipid bodies: β-carotene quantification. *Journal of Applied Phycology*, *24*(3), 541–546.

Pradana, Y. S., Sudibyo, H., Suyono, E. A., Indarto, & Budiman, A. (2017). Oil algae extraction of selected microalgae species grown in monoculture and mixed cultures for biodiesel production. *Energy Procedia*, *105*, 277–282.

Premanandh, J., Priya, B., Teneva, I., Dzhambazov, B., Prabaharan, D., & Uma, L. (2006). Molecular characterization of marine cyanobacteria from the Indian subcontinent deduced from sequence analysis of the phycocyanin operon (*cpcB-IGS-cpcA*) and 16S-23S ITS region. *Journal of Microbiology*, *44*(6), 607–616.

Presting, G. G. (2006). Identification of conserved regions in the plastid genome: Implications for DNA barcoding and biological function. *Canadian Journal of Botany*, *84*(9), 1434–1443.

Rastogi, R. P., Sinha, R. P., & Incharoensakdi, A. (2014). The cyanotoxin-microcystins: Current overview. *Reviews in Environmental Science and Bio/Technology*, *13*(2), 215–249.

Raven, P. H., Evert, R. F., & Eichhorn, S. E. (1999). *Biology of plants* (6th ed.). New York, US: W. H. Freeman and Company.

Reverté, L., Soliño, L., Carnicer, O., Diogène, J., & Campàs, M. (2014). Alternative methods for the detection of emerging marine toxins: Biosensors, biochemical assays and cell-based assays. *Marine Drugs*, *12*(12), 5719–5763.

Řezanka, T., Dor, I., Prell, A., & Dembitsky, V. M. (2003). Fatty acid composition of six freshwater wild cyanobacterial species. *Folia Microbiologica*, *48*(1), 71–75.

Rodriguez-Mozaz, S., Lopez de Alda, M. J., & Barceló, D. (2007). Advantages and limitations of on-line solid phase extraction coupled to liquid chromatography-mass spectrometry technologies versus biosensors for monitoring of emerging contaminants in water. *Journal of Chromatography A*, *1152*(1–2), 97–115.

Rozas, J. (2009). DNA sequence polymorphism analysis using DnaSP. In D. Posada (Ed.), *Bioinformatics for DNA sequence analysis* (pp. 337–350). New York, US: Humana Press.

Samorì, C., Torri, C., Samorì, G., Fabbri, D., Galletti, P., Guerrini, F., ... Tagliavini, E. (2010). Extraction of hydrocarbons from microalga *Botryococcus braun*i with switchable solvents. *Bioresource Technology*, *101*(9), 3274–3279.

Saw, J. H. W., Schatz, M., Brown, M. V., Kunkel, D. D., Foster, J. S., Shick, H., ... Donachie, S. P. (2010). Cultivation and complete genome sequencing of *Gloeobacter kilaueensis* sp. nov., from a lava cave in Kilauea Caldera, Hawai'i. *PLOS ONE*, *8*(10), 1–12.

Schmidt, R., Griesbaum, K., Behr, A., Biedenkapp, D., Voges, H. W., Garbe, D., … Höke, H. (2014). Hydrocarbons. In *Ullmann's encyclopedia of industrial chemistry* (pp. 1–74). Weinheim, Germany: Wiley-VCH Verlag.

Shakeel, T., Fatma, Z., Fatma, T., & Yazdani, S. S. (2015). Heterogeneity of alkane chain length in freshwater and marine cyanobacteria. *Frontiers in Bioengineering and Biotechnology*, *3*(34), 1–10.

Sharmila, S., Jeyanthi Rebecca, L., Anbuselvi, S., Kowsalya, E., Kripanand, N. R., Tanty, D. S., ... Swathy Priya, L. (2016). GC-MS analysis of biofuel extracted from marine algae. *Der Pharmacia Lettre*, *8*(3), 204–214.

Sherwood, A. R., & Presting, G. G. (2007). Universal primers amplify a 23S rDNA plastid marker in eukaryotic algae and cyanobacteria. *Phycological Society of America*, *43*(3), 605–608.

Sim, Y. J. (2015). *Control of toxin-producing cyanobacterial population using selected agricultural wastes* (Master's dissertation, Universiti Sains Malaysia, Penang, Malaysia). Retrieved on August 11, 2019 from http://eprints.usm.my/30537/

Smith, J. L., Boyer, G. L., & Zimba, P. V. (2008). A review of cyanobacterial odorous and bioactive metabolites: Impacts and management alternatives in aquaculture. *Aquaculture*, *280*(1-4), 5–20.

Smulko, J., Wróbel, M. S., & Barman, I. (2015). Noise in biological Raman spectroscopy. *2015 International Conference on Noise and Fluctuations (ICNF)*. doi: 10.1109/ICNF.2015.7288562

Spolaore, P., Joannis-Cassan, C., Duran, E., & Isambert, A. (2006). Commercial applications of microalgae. *Journal of Bioscience and Bioengineering*, *101*(2), 87–96.

Stanier, R. Y., Kunisawa, R., Mandel, M., & Cohen-Bazire, G. (1971). Purification and properties of unicellular blue-green algae (order Chroococcales). *Bacteriological Reviews*, *35*(2), 171–205.

Sundholm, E. (2009). *Substrate cleaning procedure*. Retrieved on August 11, 2019 from https://physics.oregonstate.edu/~tatej/TateLabWiki/lib/exe/fetch.php?media=substrate:sundholm2009_wager_ece_student_.doc

Tan, S. (2010). *Standard operating procedure: Renishaw inVia micro-Raman microscope*. Retrieved on August 11, 2019 from https://www.nano.pitt.edu/sites/default/files/safety_files/guides/Guide%20to%20Operating%20Renishaw%20inVia%20Micro%2008-18-2011.pdf

Tillett, D., Dittmann, E., Erhard, M., von Döhren, H., Börner, T., & Neilan, B. A. (2000). Structural organization of microcystin biosynthesis in *Microcystis aeruginosa* PCC7806: An integrated peptide-polyketide synthetase system. *Chemistry & Biology*, *7*(10), 753–764.

Wang, L., Min, M., Li, Y., Chen, P., Chen, Y., Liu, Y., ... Ruan, R. (2009). Cultivation of green algae *Chlorella* sp. in different wastewaters from municipal wastewater treatment plant. *Applied Biochemistry and Biotechnology*, *162*(4), 1174–1186.

Watson, S. B., Whitton, B. A., Higgins, S. N., Paerl, H. W., Brooks, B. W., & Wehr, J. D. (2015). Harmful algal blooms, In J.D. Wehr, R.G. Sheath & J.P. Kociolek (Eds.), *Freshwater algae of North America: Ecology and classification* (2nd ed.). (pp. 873–920). Cambridge, US: Academic Press.

Whitton, B. A., & Potts, M. (2012). Introduction to the cyanobacteria. In B.A. Whitton (Ed.), *Ecology of cyanobacteria II*: *Their diversity in space and time* (pp. 1–13). Dordrecht, Germany: Springer Science & Business Media.

Zhang, H., Tang, Y., Zhang, Y., Zhang, S., Qu, J., Wang, X., ... Liu, Z. (2015). Fucoxanthin: A promising medicinal and nutritional ingredient. *Evidence-Based Complementary and Alternative Medicine*, *2015*, 1–10.